

Alma Mater Studiorum Università di Bologna  
Archivio istituzionale della ricerca

The effect of vegetation in outdoor thermal comfort in archaeological area  
in urban context

This is the final peer-reviewed author's accepted manuscript (postprint) of the following publication:

*Published Version:*

Kristian Fabbri, A.U. (2020). The effect of vegetation in outdoor thermal comfort in archaeological area in urban context. BUILDING AND ENVIRONMENT, 175, 1-23 [10.1016/j.buildenv.2020.106816].

*Availability:*

This version is available at: <https://hdl.handle.net/11585/772705> since: 2020-09-25

*Published:*

DOI: <http://doi.org/10.1016/j.buildenv.2020.106816>

*Terms of use:*

Some rights reserved. The terms and conditions for the reuse of this version of the manuscript are specified in the publishing policy. For all terms of use and more information see the publisher's website.

This item was downloaded from IRIS Università di Bologna (<https://cris.unibo.it/>).  
When citing, please refer to the published version.

(Article begins on next page)

This is the accepted manuscript of:

Fabbri, Kristian, Andrea Ugolini, Alessia Iacovella and Anna Paola Bianchi. "The effect of vegetation in outdoor thermal comfort in archaeological area in urban context." *Building and Environment*, 175, 2020: 1-23.

The final publication is available at <https://doi.org/10.1016/j.buildenv.2020.106816>

Terms of use: This work is licensed under Attribution-NonCommercial-NoDerivatives 4.0 International. To view a copy of this license, visit

<http://creativecommons.org/licenses/by-nc-nd/4.0/>

This item was downloaded from IRIS Università di Bologna (<https://cris.unibo.it/>)

**When citing, please refer to the published version.**

## ***The effect of vegetation in outdoor thermal comfort in archaeological area in urban context***

### **Authors:**

Kristian Fabbri, Adjunct Professor, Department of Architecture, University of Bologna, Italy,  
[kristian.fabbri@unibo.it](mailto:kristian.fabbri@unibo.it)

Andrea Ugolini, Associate Professor, Department of Architecture, University of Bologna, Italy,  
[a.ugolini@unibo.it](mailto:a.ugolini@unibo.it)

Alessia Iacovella, Architecture graduate, Department of Architecture, University of Bologna, Italy,  
[alessia.iacovella@studio.unibo.it](mailto:alessia.iacovella@studio.unibo.it)

Anna Paola Bianchi, Architecture graduate, Department of Architecture, University of Bologna, Italy,  
[annapaola-bianchi@libero.it](mailto:annapaola-bianchi@libero.it)

### **Abstract**

The characteristics of the outdoor microclimate influence directly the outdoor thermal comfort that depends on surface reflectance, green albedo, trees, buildings, sky view factors, etc. Several researches and studies about outdoor microclimate examine area of cities, districts, squares, streets, parks, etc. and a proportion of this research studies is about the effect of outdoor microclimate on people thermal comfort, e.g. measure following Physiological Equivalent Temperature (PET). Thermal comfort in outdoor spaces has the crucial role of guaranteeing a comfortable staying in public places (such as squares, parks, etc.), as without thermal comfort people won't stay in such places. For this reason, research on tourism focuses more on outdoor thermal comfort than on indoor thermal comfort (e.g. in museum). Designing archaeological sites is very interesting and complex, since it's possible to study different scenarios and themes, together with strategies focused on solving and enhancing specific situations. Those, indeed, can vary: archaeological areas can be seen both as an exhibition area – focusing more on its relics and their correct preservation – or as an outdoor space – focusing more on the outdoor comfort, not just for the area itself but for the visitors too. In this paper we therefore report a thermal comfort and microclimate case study considering how the transformation of the urban area that surrounds an archaeological site could improve the outdoor comfort for tourists. This study uses the ENVI-met software to reproduce the actual area and six scenarios based on different urban modifications of said area: thermal variables such as air temperature, relative humidity, surface temperature and PET are considered to understand if said changes can have a positive or negative impact on thermal comfort for tourists. Comparing real and simulated data we get to focus on the scenarios with the most positive impact, in order to understand how the city could change to improve the presence of tourists in the area and what are the key elements to reach the outdoor comfort.

### **Keywords**

Outdoor microclimate map; outdoor comfort; tourist comfort; archaeological area; vegetation; ENVI-met, PET.

### **1 Introduction and literature**

Studying archaeological areas relies on a multidisciplinary approach, focused mainly on history and archaeology but also on architecture, restoration, and the exposure, preservation and use of the area itself. There are energetic, environmental and microclimatic relations between archaeological artefacts, and those have a crucial role, especially when archaeological areas are located in an urban context. Therefore, studying archaeological areas can be considered part of the building science and physics, and of the studying of solutions for mitigation of environmental effects and improving of sustainable-built environments. The use of vegetation reduces phenomena such as urban heat island and overheating and cuts down the energy requirements needed for summer cooling by decreasing the outside temperatures and solar intakes.

The relationship between building and environment and building and energy, in an outdoor space, is so peculiar to be considered a cutting-edge case study, along with the role played by vegetation.

In an archaeological area, vegetation can influence the preservation of the remains and the thermal comfort of its visitors: while it's true that an uncontrolled presence of plants can damage the ruins – e.g. causing decohesion, a natural process caused by organisms and microorganisms, or root-caused damages -, it can also have a beneficial effect regarding the outbreak of alterations phenomena – as maintained in UNI 11182 [1][2], therefore helping by preserving the ruins from solar radiation and by taking advantage of the positive effects of wind.

Below, a short literature review to support the theories presented above: we decided to divide it by topics, both to underline the multidisciplinary approach needed to study this case and to make it easier for the reader to identify the different scientific areas involved. In this way it's also clearer how our study can help those scientific areas by adding more knowledge to the gaps in the actual scientific literature.

### *1.1 Literature about the role of vegetation*

In researches about the outdoor thermal comfort and design of open spaces (parks, squares, etc.), vegetation plays a key role in mitigating the incident solar radiation and regulating the amount of water vapour in the air thanks to evapotranspiration phenomena. Literature about this topic is vast, we report here significant articles.

The research study by Morakinyo, K. Lau and C. Ren [3] analyses, through the use of ENVI-met, the thermal and energy benefits in a neighbourhood with a Greenery Coverage Ratio (GCR) of 7.2%, compared to recommended 30%. The area characterized by "very hot" thermal sensation is reduced from 60% to 50%, with 7.2% GCR, and to 17-21% with 30% GCR. Energy consumption also shows improvements in cooling data: they are reduced to 1500 kWh a day with the current GCR and to 1900–3000 kWh with GCR of 30%. The leaf area index was one of the most influencing factors on the observed benefits.

Another research by M. Fahmy, S. Sharples and M. Yahiya [4], carried out in Cairo and shows how large built surfaces and lack of a structured plan for vegetation can increase problems connected to heat and thermal stress. Using ENVI-met, they performed simulations on the hottest summer day and calculated the Leaf Angle Distribution (LAD) – the vertical distribution of the leaf surface. They managed to improve climatic conditions by introducing specific kind of trees thanks to the shadow they provided.

In urban spaces used for recreational and social activities, it may be useful to increase the wooden and grassy areas in order to improve the outdoor comfort and to invite the citizens to benefit from said spaces. Hypothetical green projects for public squares were studied by T. Zolch, M. Rahman and E. Pfeleiderer [5] using ENVI-met and observing the values of Physiologic Equivalent Temperature (PET) [6][7] reached on a hot summer day. The number of trees and their location, alongside the extension of the grassy areas, can offer a greater shaded area and reduce heat storage.

L. Zhang, Q. Zhan and Y. Lan [8] examined the influence of vegetation on the microclimate in Wuhan considering tree placement, Leaf Area Index (LAI), width of the crown and height of the tree: tall examples, with high LAI values and a large crown diameter, are preferred in outdoor design.

Another important study that uses ENVI-met to show how the increased number of trees, the density of their foliage and the use of high albedo materials can influence the outdoor microclimate belongs to M. F. Shahidan [9]. A study by Wiebke W. Klemm [10] taking place in green areas of Utrecht, shows the effects of the outdoor thermal comfort during a day, through a comparison of interviews and data measured by local weather stations. Finally, the studies of X. Yang [11] and F. Salata [12] deserve to be mentioned, both carried out using ENVI-met.

Another useful technique to reduce heat island phenomena is the use of cool materials: they have high solar reflectance and reduce surface temperatures. G. Battista, E. Carnielo and R. De Lieto Vollero [13] studied a group of buildings in the Ostiense district (Rome), using three simulation models made with ENVI-met, characterized by different percentages of green and built surfaces, proving that the one with an increased amount of solar reflectance surfaces was the most favourable.

### *1.2 Literature about tourist comfort and outdoor thermal comfort simulation*

The perception of thermal comfort in historical and archaeological sites is another important aspect of the study of outdoor areas. A research led by S. Shooshtarian [14] shows the inability to explain how thermal comfort can be achieved using traditional methods: his aim is to provide an explanatory tool and to move

from literature to theoretical frameworks in order to understand better the comfort-related data, especially regarding outdoor environments.

Tourists are highly influenced by climate: it can affect the destination choice and the travel program. A study, carried out in Kerman during summertime, by S. Zare, N. Hasheminezhad and K. Sarebanzadeh [15] uses both subjective and objective procedures to evaluate climate perception by tourists: they presented a questionnaire to tourists on one hand and used the RayMan software on the other. As a result, the subjective Predicted Mean Vote (PMV) value was higher than the objective one, due to visitors' dissatisfaction with local climate, since they weren't used to it. We can therefore see that objective and subjective procedures can be useful to determine the outdoor thermal perception, and could be used as a further validation of the obtained data.

The transient Acceptable Temperature Range (ATR) is a subjective method of comfort evaluation, and it consists of a temperature range considered satisfying by over 80% of the users in questionnaires on outdoor comfort: users had to determine whether the environment was satisfying or not during the questionnaire submission. An alternate method was proposed by P. Cheung and C. Jim [16] in their study set in Hong Kong, where users were required to answer the questionnaire for a whole hour, in order to develop heat exchanges between humans and environment, demonstrating that more reliable results were achieved.

### *1.3 Literature about conservation of archaeological landscapes*

The lifespan of a monument is connected to the environment in which it is located and it is influenced by spontaneous vegetation or planned plant structures. The fear of not being able to manage plant dynamics has led in the past to an "aseptic sterilization" of archaeological sites. On one hand spontaneous flora can accelerate phenomena of deterioration (micro/macro de-cohesion of substrates, mechanical damage caused by roots, chemical alterations, etc.), but, on the other hand, controlled vegetation can contribute to define the microclimate of archaeological sites, making it an important source of biodiversity, especially in urban contexts.

The presence of plants constitutes an element of defense against environmental factors (solar radiation, wind, precipitation, pollutants, marine aerosol) and offers shading, reduction of thermal excursions and design for the architectural reading of the area. Plants can be classified in relation to their dangerousness for archaeological sites [17]; the archaeological park of Selinunte, an ancient Greek city on the south-western coast of Sicily [18], is an example of interdisciplinary work based on the conservation of natural environments where the dynamics of vegetation and archaeological ruins were balanced; controlled management of vegetation should be studied in the design phase, choosing species with known characteristics, suitable for the site. Vegetation can also help in reconstructing the image of the archaeological site from a historical point of view.

### *1.4 Literature about microclimate and archaeological areas*

Research of X. Luo [19][20] on thermal comfort in archaeological areas, specifically about the microclimate that could suit archaeological relics located above the ground, after excavations and contribute in their correct conservation. It's clear that relics need a microclimate different from what would be comfortable for visitors, since it'd better to recreate the underground situation, with low temperatures and high humidity.

Fabbri and Ugolini [21] studied the same topic alongside with the role of vegetation in an outdoor archaeological area: they studied three different hypothetical situations: absence of vegetation, presence of homogeneous vegetation (same kind of trees) and presence of heterogeneous vegetation. As a result, the presence of vegetation near archaeological ruins doesn't just reduce the risk of thermal shock near the area, but also keeps the relative humidity level more adequate for the preservation of ruins, as well as protect the area from winds.

## **2 Aim of research**

This article research focuses on the study of an archaeological area located in an urban context: we used different configurations of both materials and vegetation, with a dual objective: on one hand to contribute

to the (few) studies about microclimate in archaeological areas, on the other to highlight the role of the percentage of green surfaces in influencing microclimatic conditions in urban contexts.

### 3 Case study

The case study is an archaeological area of the roman amphitheatre of Rimini (coordinates GIS: 44.060326, 12.575293), located in the city walls, in a peripheral position if compared to the inner city.

Rimini, located in northern-central Italy, is a seaside town, characterized by a humid subtropical climate, with hot summers and mild winters (CFA Koppen-Geiger classification [22][23]).

According to the meteoblue website [24], winter daily mean temperatures are 3°C as minimum and 10°C as maximum; during summer they vary from 18°C as minimum to 31° as maximum. The coldest months are usually January and February (maximum temperatures can be slightly lower than 0° C), while the hottest ones are July and August (with maximum temperatures rising up to more than 35° C). In those periods there are also, respectively, clouded skies with few sunny days and mostly sunny days with few clouds. Spring is usually the most rainy time of the year, with a peak in April, but the climate is generally characterized by dry days. Dominant winds come from N-NE, NE with maximum speed higher than 61 km/h, and from E-NE, with maximum speed over than 50 km/h.

The roman amphitheatre of Rimini (*figure 1.a*) was built in the II century A.D. to celebrate gladiator games, but in III century AD was already abandoned, incorporated in the city walls system and partly buried. In 1926 a part of the building was brought back to light and restored [25][26].

Nowadays (*figure 1.b*) we can only see around half of the original building, since the other part is still buried and a kindergarten, the Italian-Swiss Educational Centre (CEIS, in Italian), is on top of it. Nearby there are the Margherita Zoebeli cycle path, two large green areas (Maria Callas park and Alcide Cervi park) and three big parking lots (Settebello parking, Ex-Padane parking and Antonio Gramsci parking). Concrete is largely used in the area, despite the big green areas.

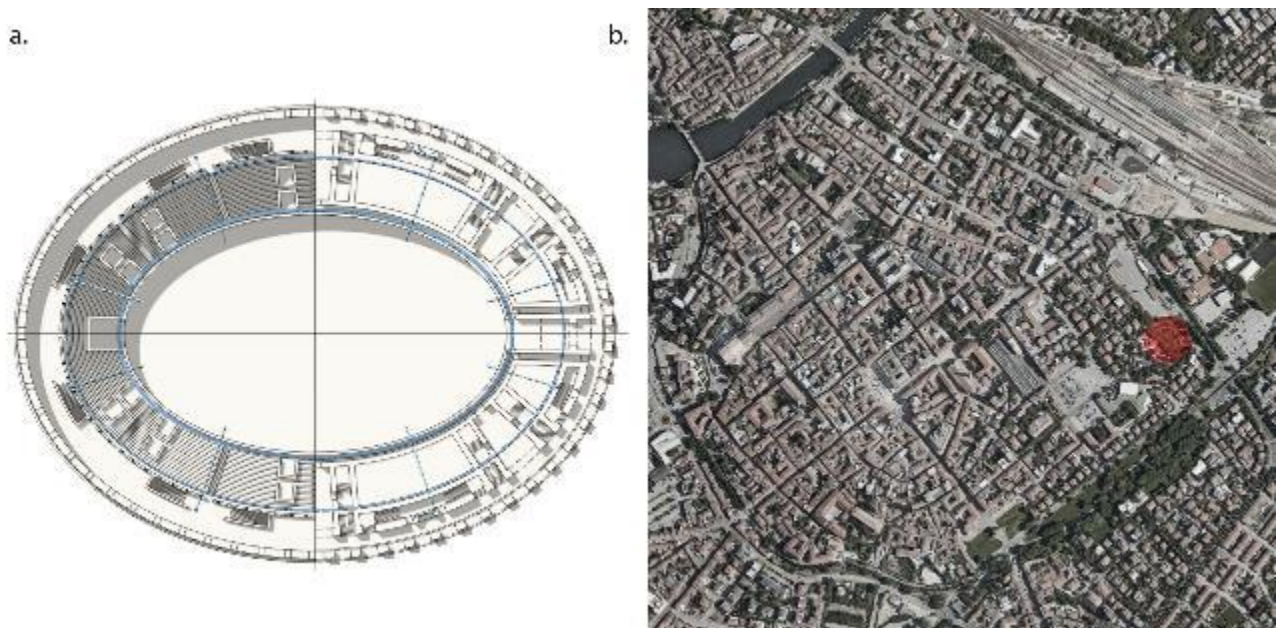


**Figure 1.** a) position of Rimini in the Italian peninsula, b) planimetry of Rimini c) actual planimetry of the amphitheatre, d) recreation of the hypothetical original aspect of the amphitheatre.

### 4 Research methodology

We applied a research methodology divided into four phases:

1. to create two microclimate models at different in scale of case study state of art;
2. to calibrate virtual models with the climate data measured locally;
3. to define some scenarios with different trees configuration and reflectance of the surfaces;

4. finally to compare the Outdoor Microclimate Maps (OMM, as defined in [27]) of the obtained results both among themselves and with the current, actual situation.

We studied the archaeological area of the amphitheatre of Rimini; we decided to use two different model sizes in order to verify the effects of vegetation both on the neighbourhood and on the area, in relation to the different scenarios and to verify the consistency of the two different-scaled models. The dimension of the boundary area has been chosen in order to avoid software miscalculations, as seen in other ENVI-met based researches on the same topic (see the scientific literature for further references). About the 3D modelling of the bushes, we created a model of bush geometrically similar to the actual one, according to the software modelling criteria.

#### *4.1 Phase 1: the two microclimatic models of the area*

The microclimatic model of the area was created using the software ENVI-met Summer V.4 [28] and portrays the actual situation of the area. The model was validated using the climate data measured by the climate station “Rimini Urbana”, provided by ARPAE Emilia-Romagna [29], verified through their digital equivalent measured by receptors placed in the software using SPACES. We decided to create two models, different in scale, in order to compare the results both for the specific, detailed model and for the larger one, that included a wider part of the urban context. The two models are consistent, since our element of interest is in a central position and the grids have the same amounts of cells in length, width and height: the only thing that varies is the dimension of said cells.

##### Area of analysis

The two areas of analysis are different in scale: the one with a larger scale (*figure 2.a*) shows a larger portion of the city, including also the large paved areas of the parkings and the green areas of the parks. The one with a closer scale (*figure 2.b*) only shows the ruins and their proximity: we can see the archaeological area, the CEIS buildings, the cycle path, some nearby buildings and part of via Roma and its trees and of the Ex-Padane parking. In both areas the amphitheatre is centred and surrounded by a protection zone, to avoid potential software miscalculations.

We used 150x150x35 cells grids (35 is the height); the cells dimension varies: in the small model is 1mx1mx1m while it's 3mx3mx3m in the large one. To efficiently compare data, we picked four receptors, A, B, C and D. Their coordinates, expressed in metres and referred to the 0,0 of the grid, are: A(222,300), B(288,333), C(210, 192), D(186,255) in the large model and A(204, 231), C(225,174) and D(159,351) in the small model. In the latter, we didn't take the receptor B in consideration, since it was placed outside the area of analysis.



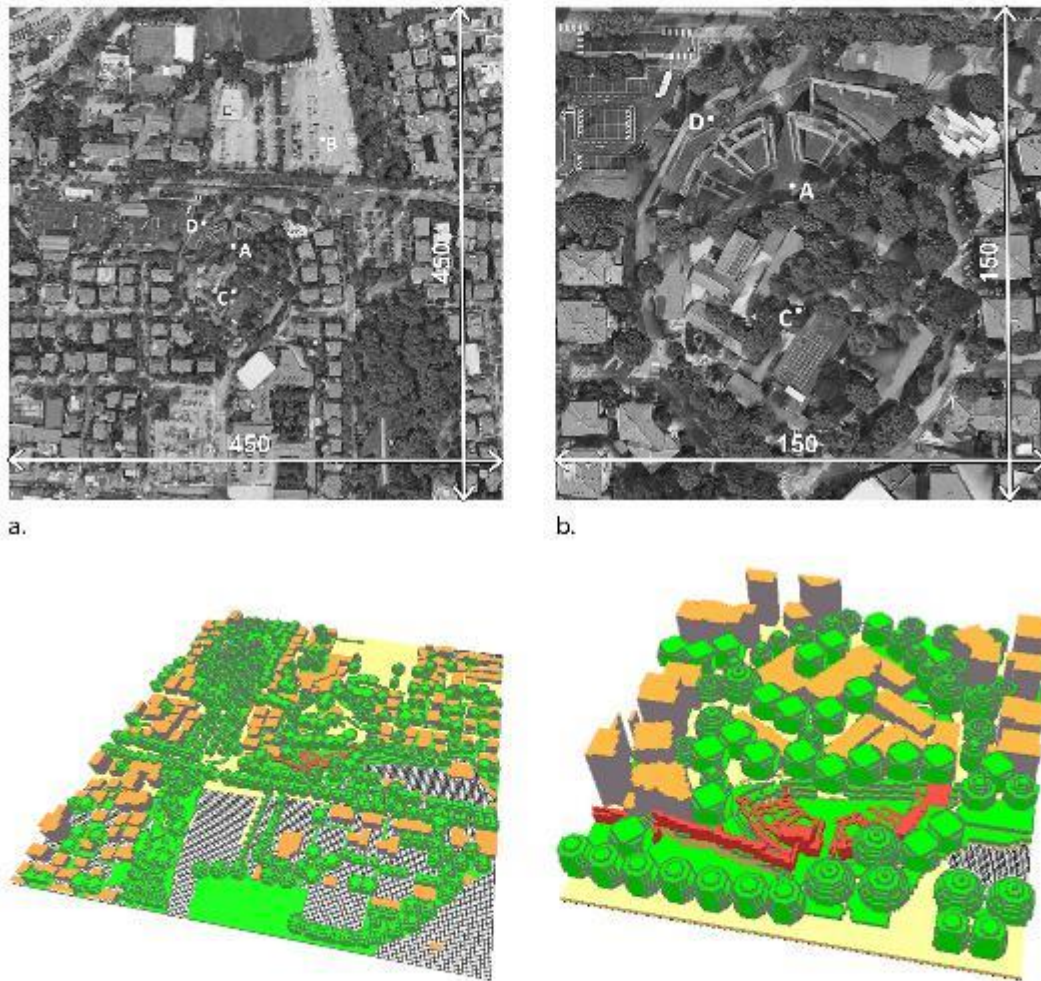


**Figure 2.** a) Large area of analysis with receptors shown. b) Small area of analysis with receptors shown.

### 3D modelling of a shrub

The project scenarios include adding hedges (see paragraph 5.3), created in ENVI-met through the creation of a 3D model of a shrub by using the modelling tool *Tree*. The hedge are characterized by deciduous leaves, roots with diameter and depth of 0,5 m, LAD = 2 and its dimensions are 1mx1mx1m.



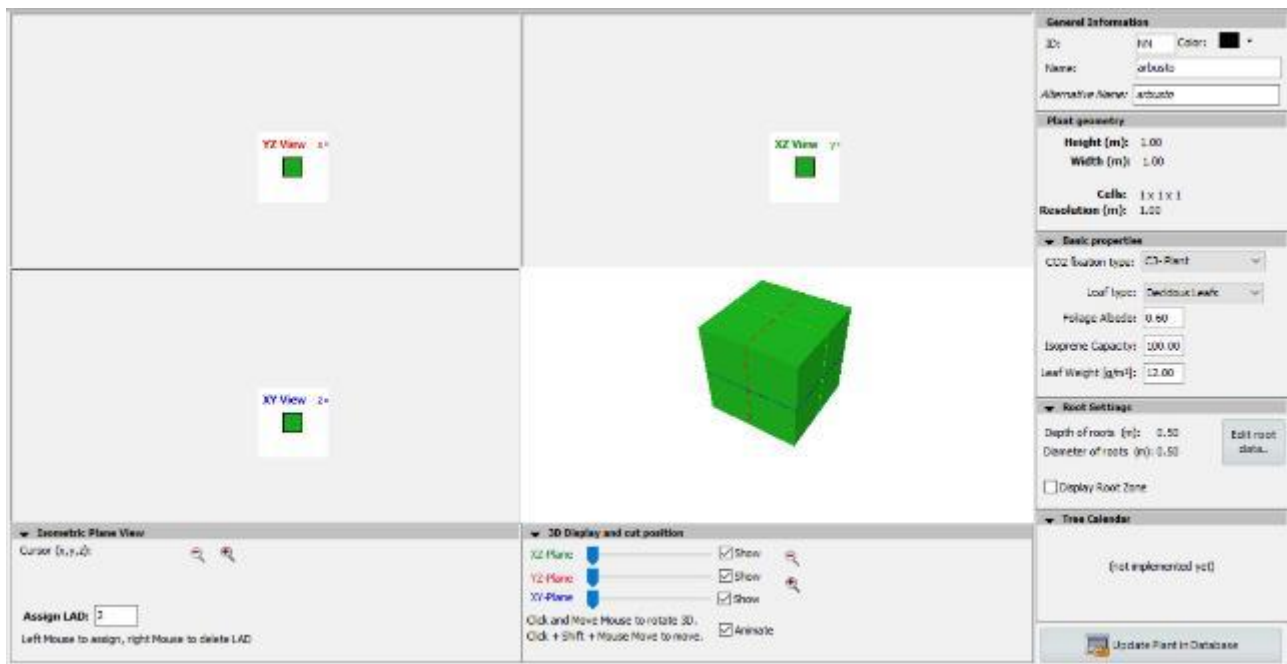


**Figure 3.** Modelling window of the new kind of vegetation in ENVI-met.

#### Climate data and boundary conditions

Since ENVI-met simulations relate to a specific day, we picked the 04<sup>th</sup> August 2017, the hottest summer day in the past decade, characterized by extreme conditions of outdoor comfort: it's interesting to analyze the worst situation possible, in order to suggest solutions that might improve the frequentation of the area. The climate data were supplied by the Rimini Weather Station [30] (Table 1).

The initial boundary conditions are:

- start date: 04.08.2017
- start time: 06:00
- simulation time: 48 h, 2<sup>nd</sup> day used for evaluation
- wind speed measure in 2 m height (m/s): 1,86 m/s
- wind direction (deg): E 97°

Table 1. Climate data 48h simulation 04/08/2017 (Rimini Weather Station)

hours	Average hourly air temperature 2m above ground (°C)	Average hourly relative humidity 2m above ground [%]
00:00	27.30	52
01:00	27.20	50
02:00	27.60	51
03:00	27.00	49
04:00	26.10	44
05:00	25.90	47
06:00	26.80	44
07:00	29.60	35
08:00	30.70	43
09:00	31.60	39
10:00	32.70	31
11:00	32.20	34
12:00	31.60	48
13:00	31.40	51
14:00	31.10	57
15:00	31.20	58
16:00	31.10	59
17:00	31.30	56
18:00	30.20	53
19:00	29.50	60

20:00	29.60	68
21:00	29.00	63
22:00	28.20	59
23:00	28.00	61
00:00	27.80	43
01:00	28.10	34
02:00	27.10	31
03:00	26.50	37
04:00	25.80	37
05:00	26.90	33
06:00	31.00	28
07:00	33.50	18
08:00	34.20	17
09:00	34.20	21
10:00	33.80	29
11:00	33.80	27
12:00	33.20	36
13:00	32.90	42
14:00	33.70	38
15:00	33.60	35
16:00	33.90	24
17:00	33.50	27
18:00	32.80	29
19:00	32.40	26
20:00	31.40	28
21:00	30.30	30
22:00	29.60	29
23:00	29.80	26

#### 4.2 Phase 2: model calibration with local measured climate data

The second phase consists of calibrating the results of the two models with the real data measured by the ARPAE weather station, related to air temperature (°C), which is the least influenced parameter by unpredictable local factors such as weather conditions, precipitations, etc.

There are reference standards to validate indoor energy consumption, *following ASHRAE Guideline [31]*, while the situation is different for outdoor environments. For the latter, the validation criteria are: (a) temporal (an actual physical point monitored for a certain number of hours); (b) spatial (more physical points monitored at the same time); (c) an intermediate criterion (multiple physical points monitored for several hours). Regarding the calibration

criteria, the literature reported in Fabbri and Costanzo's article [32] can be used as reference.

We picked the temporal criterion, using one receptor of the model (identified as Receptor A), placed in cells 74;100 in the large model and in cells 68;77 in the small one, as physical reference point.

We then compared the mean temperature values obtained by Dexter with those simulated regarding the 4<sup>th</sup> August 2017, from 01:00 to 23:59 (*Table 2*).

*Table 3 shows the results calibration of the measured data with the simulated ones. Table 4 shows the calibration between large and small area. Both models are calibrated.*

Table 2. Measured and simulated data:

hours	air temperature (measured by ARPAE)	air temperature (simulated) in Receptor A LARGE MODEL	air temperature (simulated) in Receptor A SMALL MODEL
01:00	27.80	28.09	27.89
02:00	28.10	28.07	27.67
03:00	27.10	27.58	26.35
04:00	26.50	27.1	26.15
05:00	25.80	26.61	25.31
06:00	26.90	26.76	25.43
07:00	31.00	28.84	27.56
08:00	33.50	30.87	29.75
09:00	34.20	32.04	30.89
10:00	34.20	32.57	31.45
11:00	33.80	32.79	31.76
12:00	33.80	32.89	32.04
13:00	33.20	32.64	32.05
14:00	32.90	32.43	31.95
15:00	33.70	32.61	32.18
16:00	33.60	32.54	32.23
17:00	33.90	32.58	32.59
18:00	33.50	32.31	32.35
19:00	32.80	31.98	31.83
20:00	32.40	31.68	41.54
21:00	31.40	31.11	30.97
22:00	30.30	30.43	30.39
23:00	29.60	29.89	28.68

Data validation was conducted following the ANSI/ASHRAE criteria, described in ASHRAE Guideline 14-2002 Measurement of Energy and Demand Savings, Ashrae [31]. We reported the MBE (Mean Bias Error) values, the CV (RMSE) (Coefficient of Variation of the Root-Mean Square Error) and the Pearson coefficient.

Table 3. Calibration between measured and simulated data

	LARGE MODEL SIMULATED DATA		SMALL MODEL SIMULATED AREA		ASHRAE GUIDELINE [31]
<b>MBE [%]</b>	6.35%	Validated	2.17%	Validated	Calibrated if MBE < 10%
<b>CV (RMSE) [%]</b>	6.97%	Validated	3.62%	Validated	Calibrated if CV(RMSE) < 30%
<b>PEARSON</b>	0.74	Strong correlation	0.97	Optimal correlation	if Pearson > 0.7 (strong correlation; 0.3-0.7 (correlation); < 0.3 (weak correlation)

Table 4. Calibration between ENVI-met large model with the small one

			ASHRAE GUIDELINE [31]
<b>MBE [%]</b>	6,35%	Validated	Calibrated if MBE < 10%
<b>CV (RMSE) [%]</b>	2.21%	Validated	Calibrated if CV(RMSE) < 30%
<b>PEARSON</b>	0.74	Strong correlation	if Pearson > 0.7 (strong correlation; 0.3-0.7 (correlation); < 0.3 (weak correlation)

#### 4.3 Phase 3: definition of the project scenarios and OMM output construction

Our research includes six simulated scenarios: three for the large model, and three for the small one. These scenarios are based on the variation of different aspects: trees configuration, which implies a positive or negative variation of the tree percentage in the scenarios; the materials, with the consequent albedo and reflectance values variation; and the elimination of some buildings in the area.

Since the 3D models realized with ENVI-met are a rather accurate representation of the actual situation, we were able to acquire further data, such as the percentage of green areas and the number of trees for each scenario. Indeed, we found the percentage of green areas by comparing the total number of the cells of the

models with the number of cells representing the green areas; the number of trees was acquired by simply counting the number of trees of each scenario.

Tables 5 and 6 show the scenarios description for each area.

Table 5. Large scenarios description

Scenarios (n.)	Description	Green area (%)	Trees (n.)	Soil and Surfaces
0 (large model)	- Current state	33%	448	Common asphalt (albedo: 0.2) Colored asphalt (albedo: 0.5) Stone paving (albedo: 0.8) Grass (albedo: 0.2) Gravel (albedo: 0.4)
1 (large model)	- Increase in green area; - Trees insertion in parking lots; - Flooring changing in parking lots.	38%	505 Fraxinus excelsior, Carpinus betulus	In parking areas: light-colored draining asphalt introduction (albedo: 0.5)
2 (large model) (*)	- CEIS buildings removal; - Ground lowering from 3.2 m to 0; - Grass introduction.	36%	418	Grass introduction (albedo 0.2)
3 (large model)	- CEIS buildings removal; - Ground lowering; - Mineral flooring introduction.	30%	418	Mineral flooring introduction (albedo 0.0)

(\*) CEIS Area-Amphitheater arena height difference: 3.2 m, in reference to the 0.00 m arena level.

Table 6. Small scenarios descriptions

Scenarios (n.)	Description	Green area (%)	Tree (n.)	Soil and Surfaces
0 (small model)	- Current state	33%	64	Common asphalt (albedo: 0.2) Colored asphalt (albedo: 0.5) Stone paving (albedo: 0.8) Grass (albedo: 0.2) Gravel (albedo: 0.4)
4 (small model)	- Hedge insertion; - Green area increase; - Trees insertion; - Compacted earth paths insertion.	32%	66 Tilia platyphyllos	Grass introduction (albedo 0.2) Compacted earth introduction (albedo 0.0)
5 (small model)	- CEIS buildings removal; - Grass introduction.	55%	64	Grass introduction (albedo 0.2)
6 (small model)	- CEIS buildings removal; - Grass introduction; - Trees removal in CEIS area.	55%	38	Grass introduction (albedo 0.2)

## 5 Results and Outdoor Microclimate Map

According to research aims, we report results related following physical variables, from each scenarios:

- *Air temperature* [ $^{\circ}\text{C}$ ]: allows to evaluate the temperature distribution to identify the presence of high values areas;
- *Relative humidity (RH)* [%]: allows to identify a wet (>65%) or dry ( $\leq 45\%$ ) environment, it can affect PET values and is influenced by green areas and trees presence;
- *Surface Temperature ( $T_{\text{surface}}$ )* [ $^{\circ}\text{C}$ ]: depends on the reflectance and albedo of the materials and on the view factor.

Moreover, we report the outdoor comfort expressed by *Physiologic Equivalent Temperature* (PET), whose range are displayed in table 7. The PET index is a biometereological parameter [33] [34] that describes

individual thermal perception and refers to human body energy balance; it is expressed in °C, and is easier to understand compared to parameters like the PMV percentage.

Table 7. PET values and Grade of physiological stress

PET (°C)	Thermal perception	Grade of physiological stress
less of 4	Very cold	Extreme cold stress
from 4 to 8	Cold	Strong cold stress
from 8 to 13	Cool	Moderate cold stress
from 13 to 18	Slightly cool	Slight cold stress
from 18 to 23	Comfortable	No thermal stress
from 23 to 29	Slightly warm	Slight heat stress
from 29 to 35	Warm	Moderate heat stress
from 35 to 41	Hot	Strong heat stress
more of 41	Very Hot	Extreme heat stress

### 5.1 OMM results for the large model scenarios

The results related to the large model scenarios are referred to four different hours: we reported the results taken every two hours (10:00, 12:00, 14:00 and 16:00), with more in-depth observation at 14:00, which is the hottest time of the day, so the worst regarding thermal comfort.

#### OMM air temperature scenarios, large model

*Scenario 0 large model:* In the early afternoon, in the parking lots we register a temperature of 40°C, 7°C higher than in the other areas; via Roma suffers from this, despite the presence of green areas, while the amphitheatre and the urban areas don't (*figure 4.a*).

*Scenario 1:* after including green areas in the parking lots, we register improvements: at 14:00, temperature is 32 – 35 °C, so 3 – 5 °C lower than the actual one. Temperature is generically lower all day long but there is no significant reduction in the CEIS and amphitheatre areas (*figure 4.b*).

*Scenario 2:* after removing the CEIS buildings and adding grass we register a temperature increase near the ruins; at 14:00 we register the worst situation, with temperature values over 38°C. The building removal creates a negative effect on the surroundings too: adding grass is not enough to reduce the high temperatures (*figure 4.c*).

*Scenario 3:* as it happens in the previous scenario, we find negative results: morning temperatures are higher than the actual ones and at 14:00 they reach 37 – 38°C in the CEIS and amphitheatre areas. The flooring changes bring negative effects in the surroundings too: in the Antonio Gramsci parking temperatures are half a degree higher and in the Alcide Cervi park the extension of the area coloured in green by the software is smaller (*figure 4.d*).

*For detailed values, see Annex, tables 8.1 and 8.2.*

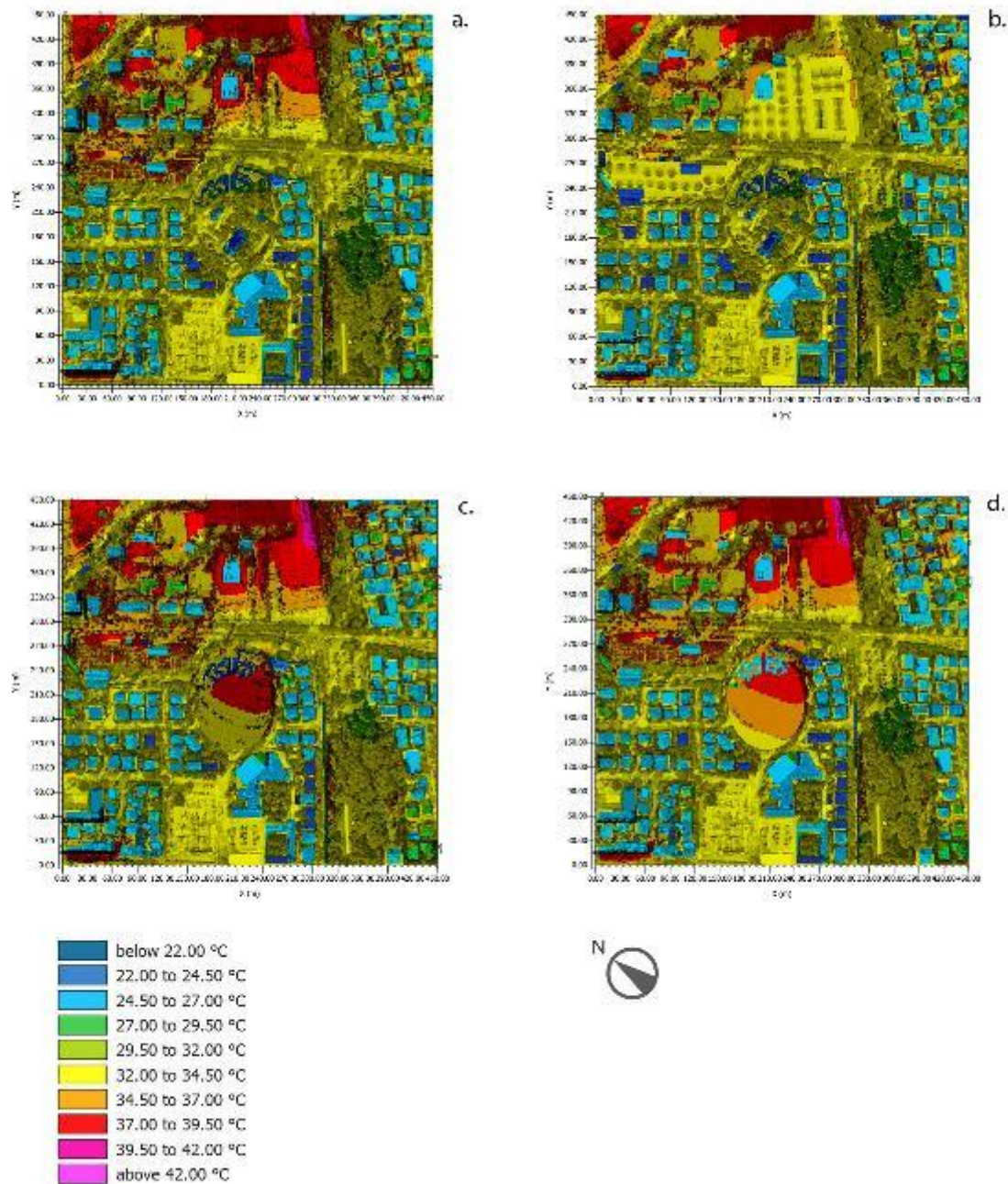


Figure 4. Large model: air temperature results at 14:00: (a) scenario 0, current state; (b) scenario 1; (c) scenario 2; (d) scenario 3.

#### OMM relative humidity scenarios, large model

*Scenario 0 large model:* a very dry air is registered since morning in the whole area. At 14:00, asphalted areas and the parking areas register 27 – 30% of RH, while in the remaining areas we get 46%, thanks to presence of green areas (*figure 5.a*). This may be due to the evaporative processes caused by a very high temperature (around 40°C).

*Scenario 1:* we register improvements since morning; at 14:00, we reach values higher than 40%, with improvements in the green areas too. There are no variations in the amphitheatre area, except for the



green area by the entrance on via Roma. Our intervention brings positive effects in parking lots, in Maria Callas park and in via Roma, but doesn't significantly affect the archaeological and CEIS areas (*figure 5.b*).

*Scenario 2:* after recording positive results in the morning, at 14:00 we register 28 -29% RH in the amphitheatre area, too little considering the 38°C temperature. Our intervention lowers the RH in the surroundings too, affecting via Roma and the parking lots (*figure 5.c*).

*Scenario 3:* as in scenario 2, we have improvements in the morning but a turnaround at 14:00. In the amphitheatre area we register 27 – 30 % RH values, lower than actual state scenario (*figure 5.d*). This might be due to higher temperatures (38°C) in scenario 3.

For detailed values, see Annex, tables 9.1 and 9.2.

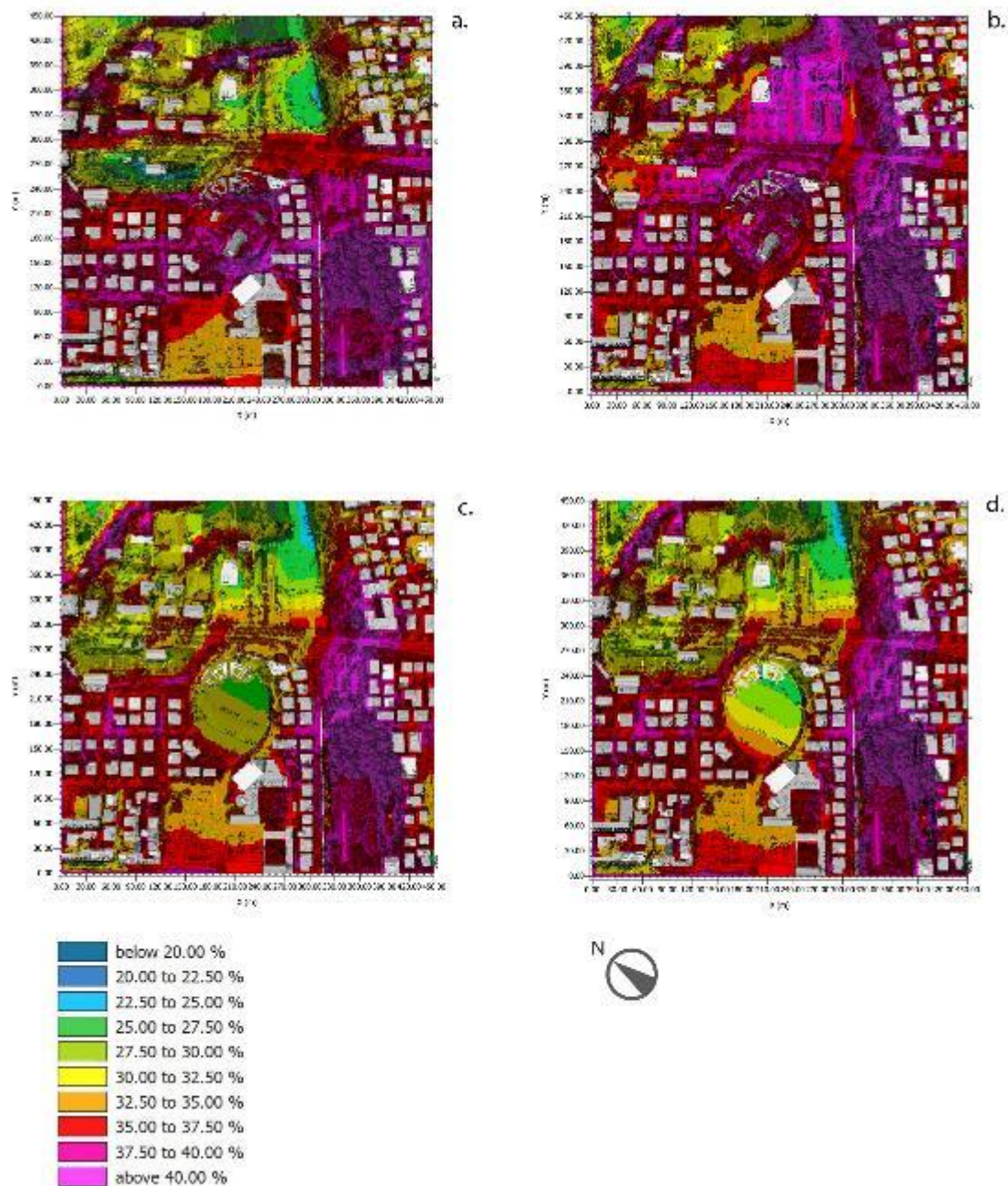


**Figure 5.** Large model: RH results at 14:00: (a) scenario 0, current state; (b) scenario 1; (c) scenario 2; (d) scenario 3.

OMM surface temperature scenarios, large model

*Scenario 0 large model:* surface temperature shows to be higher in parking areas than in built ones, reaching 58°C at 14:00. In asphalted streets we recorded 38 – 42°C, while in green areas the values are 30°C lower than those of the large paved areas. We report lower temperatures near the trees of urban courts (figure 6.a).

*Scenario 1:* we report clear improvements – in early afternoon we register around 38°C in the less shaded areas of the parking lots, much better than the current situation. Neither via Roma nor the archaeological area are affected (figure 6.b).

*Scenario 2:* temperature rise in the amphitheatre and CEIS areas – at 14:00 it reaches 46 °C in the archaeological area. This proves the positive effect of the current existing trees, that allow lower surface temperatures (figure 6.c).

*Scenario 3:* similarly to scenario 2, our intervention has a negative impact on surface temperatures – inserting mineral pavements causes temperatures higher than those of the previous scenario. At 14:00 we reach 43°C in the archaeological area (figure 6.d).

*For detailed values, see Annex, Tables 10.1 and 10.2.*

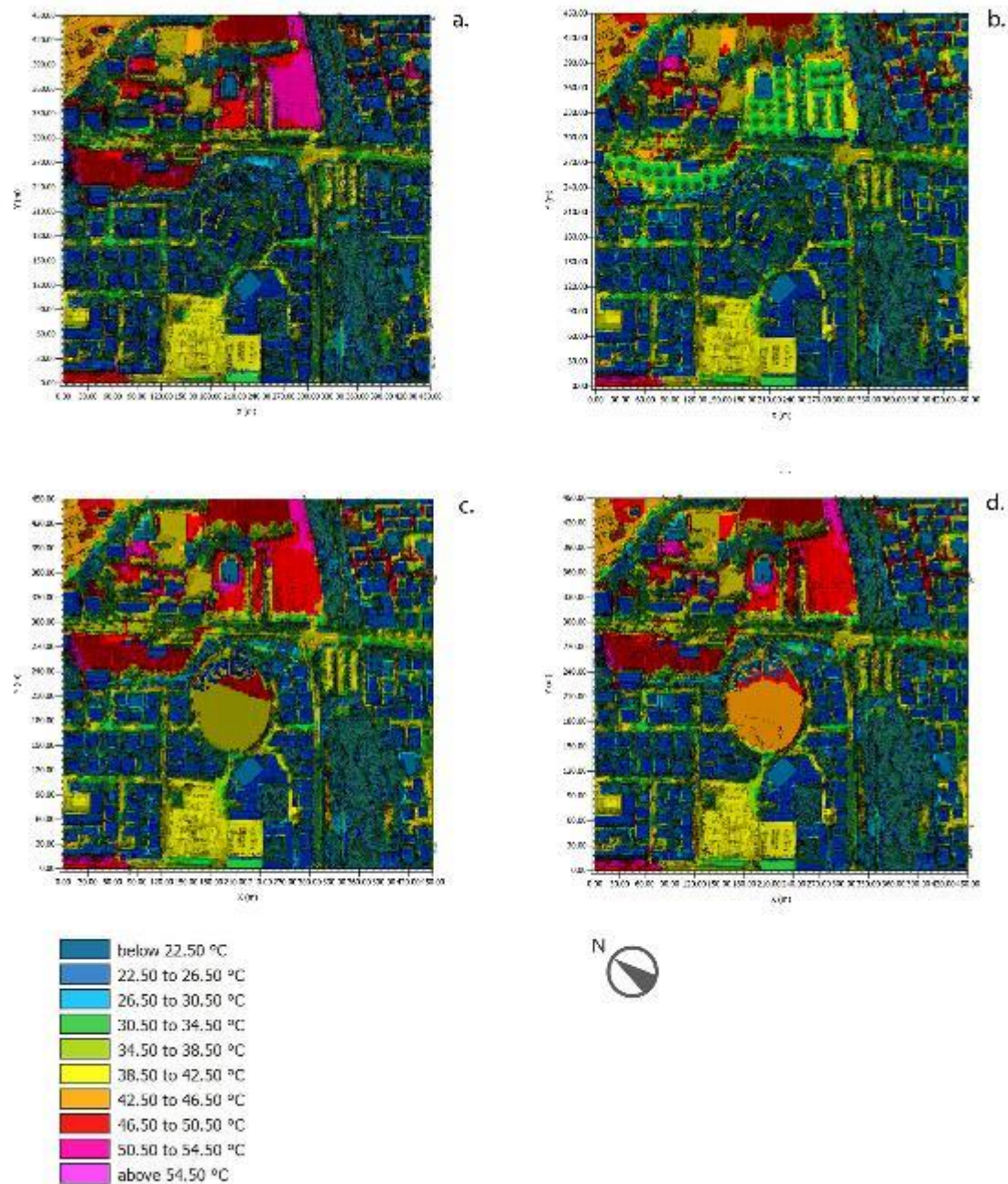


**Figure 6.** Large model: surface temperature results at 14:00: (a) scenario 0, current state; (b) scenario 1; (c) scenario 2; (d) scenario 3.

#### OMM PET scenarios, large model

**Scenario 0 large model:** parking lots in the early afternoon register 40°C, 7°C higher than the other areas; via Roma, despite the presence of vegetation, suffers from it, while the amphitheatre area and the urban centre don't (figure 7.a).

**Scenario 1:** at 14:00, PET values are 34 - 38°C, thermal perception is *warm and moderate stress*, better than the current situation of *extreme thermal stress*. Our project improves the parking lot situation, but doesn't

affect the surroundings: the amphitheatre area still registers around 34°C (*moderate heat*), hardly usable by visitors (*figure 7.b*).

*Scenario 2:* our project doesn't bring any improvement – in the morning, the amphitheatre and CEIS areas record higher PET values than those of the current state. At 14:00, we reach values above 50°C (*very hot and maximum stress*) close to the ruins. CEIS area gets worse too, reaching 43°C PET (*very hot*) (*figure 7.c*).

*Scenario 3:* our project has a negative effect – PET values are higher than those of the current state and of scenario 2 since morning. At 14:00, the areas closer to the ruins reach PET values higher than 50°C, while in CEIS area we reach 43°C PET, similarly to scenario 2. There are no significant variations in the urban context (*figure 7.d*).

*For detailed values, see Annex, Tables 11.1 and 11.2.*



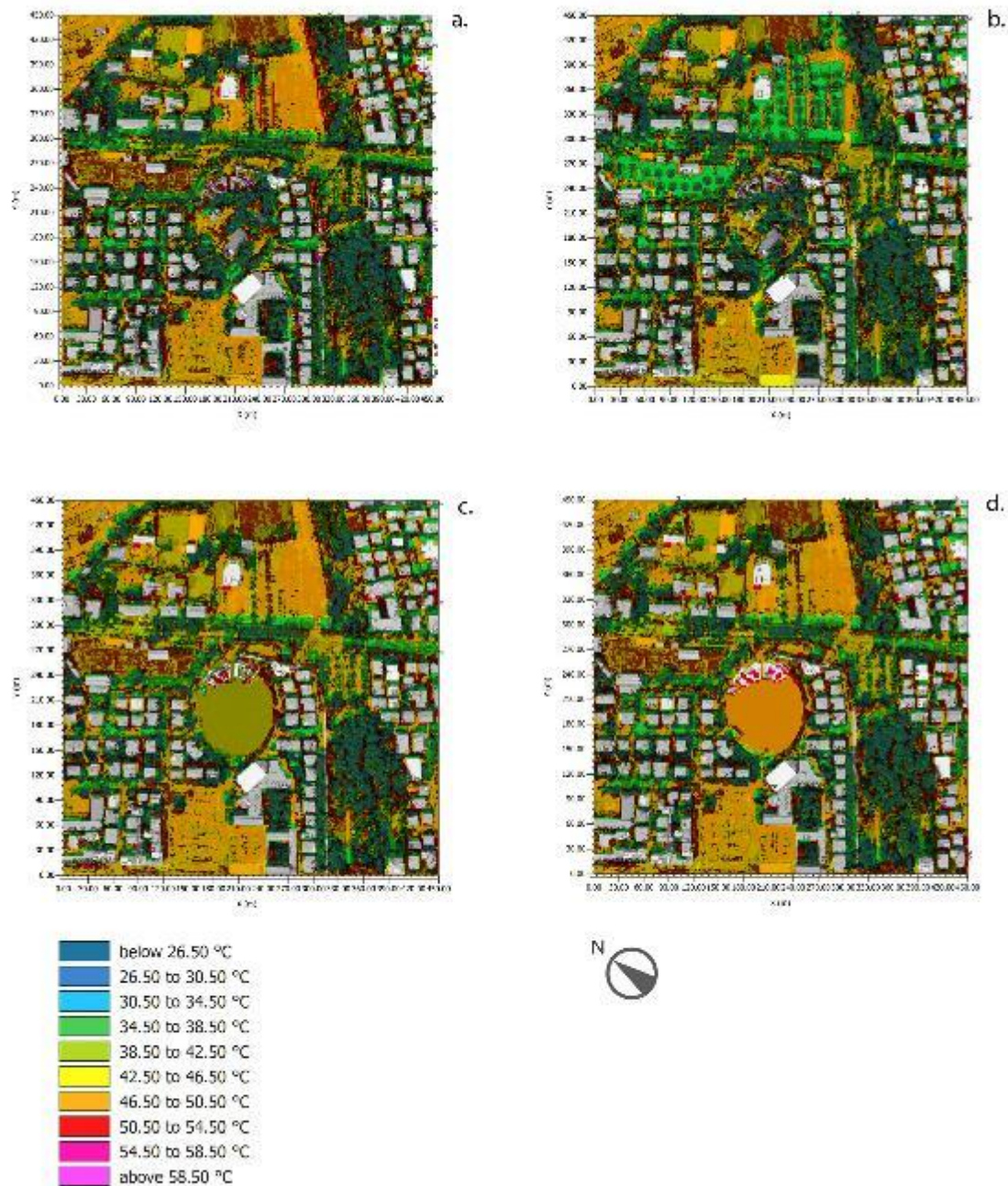


**Figure 7.** Large model: PET results at 14:00: (a) scenario 0, current state; (b) scenario 1; (c) scenario 2; (d) scenario 3.

## 5.2 OMM results small model

Similarly in same way of previous paragraphs, for the small model scenarios, we report results for four hours, taken every two hours (10:00, 12:00, 14:00, 16:00), with more in-depth observations at 14:00.

### OMM air temperature scenarios, small model

*Scenario 0 small model:* 35°C are reached in the early afternoon in the parking lot and in via Vezia, while in the amphitheatre area the prevailing temperature is 32°C, except for some red-coloured areas with values

higher than 33°C. The green areas surrounding the CEIS area mitigate the temperatures, protecting the archaeological area from the heat wave (*figure 8.a*).

*Scenario 4:* we register slightly lower temperatures along the cycle path, maintained all day long; at 14:00, along the paths of compacted earth, created inside the archaeological area, temperatures rise of around 1°C (*figure 8.b*).

*Scenario 5:* the elimination of CEIS buildings and the grass introduction lead to positive effects – at 14:00 we don't see any red-coloured area ( $T > 33.50^{\circ}\text{C}$ ) along the remaining amphitheatre walls, and we register 32°C near the trees located in the CEIS area. The green-coloured areas, corresponding to milder temperatures, increase their dimensions (*figure 8.c*).

*Scenario 6:* after the elimination of both CEIS buildings and trees, near the ruins the temperatures rise since morning. At 14:00 the CEIS area maintains the same temperatures of the current state (32 - 33°C), while near the ruins there are more red-coloured areas, signalling temperatures around 34°C (*figure 8.d*).

*For detailed values, see Annex, Tables 12.1 and 12.2.*



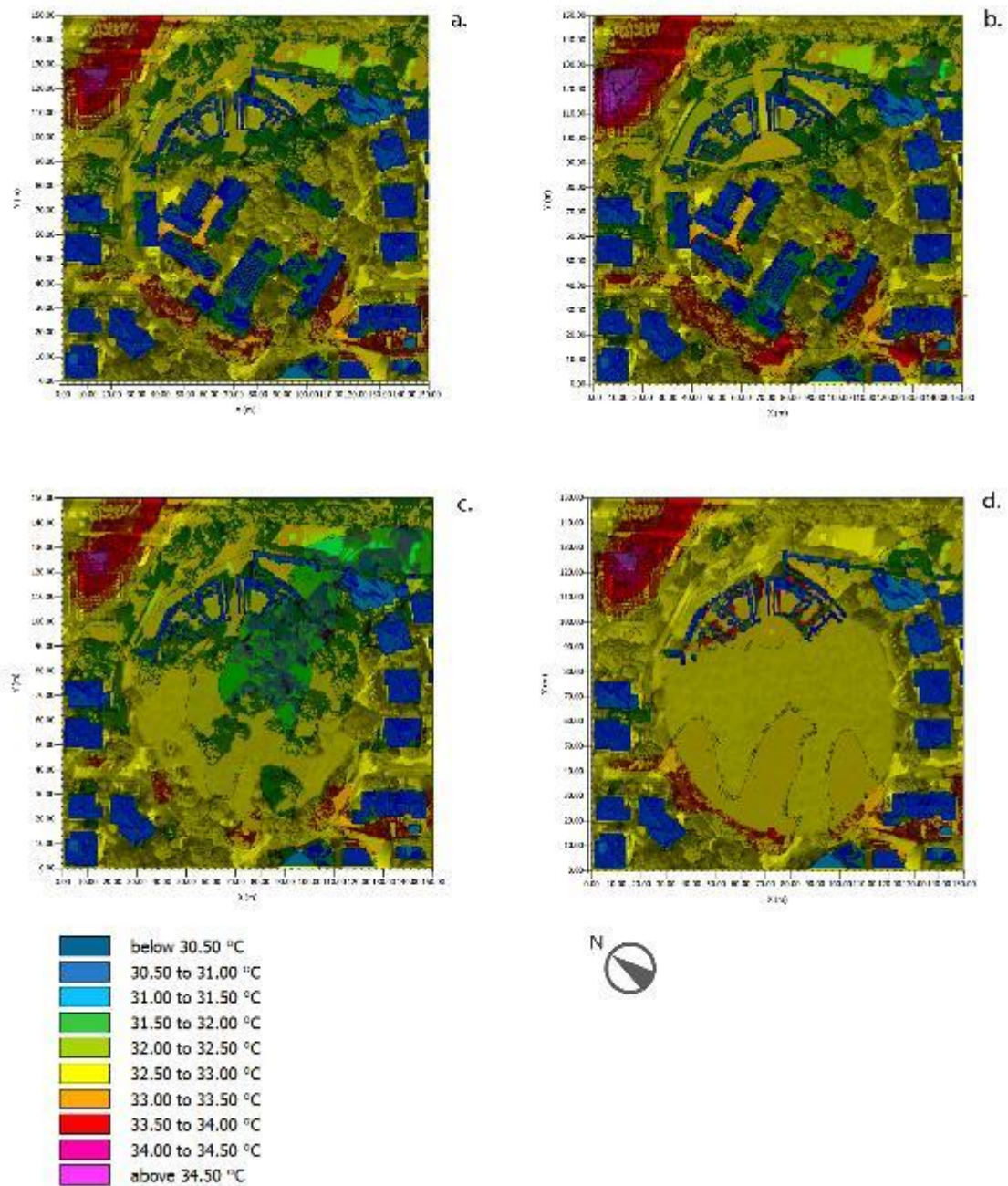


**Figure 8.** Small model: Air temperature results at 14:00: (a) scenario 0, current state; (b) scenario 4; (c) scenario 5; (d) scenario 6.

#### OMM relative humidity scenarios, small model

**Scenario 0 small model:** at 14:00 we register RH values above 37%, so still low. The vegetation in the area isn't enough to reach comfortable RH levels (figure 9.a).

**Scenario 4:** there are no significant changes compared to the current situation; at 14:00 we reach values higher than 37%, maintaining low values and a generally dry condition. There is a slight increase in RH values alongside the inserted hedge (figures 9.b).

*Scenario 5:* RH reaches higher values after the grass insertion; At 14:00 we register values higher than 37%, whereas the current ones are 35 - 37%. This goes on throughout the whole afternoon, with RH improving in the CEIS area (*figure 9.c*).

*Scenario 6:* similarly to scenario 5, we register positive effects; at 14:00 the dimension of the areas signalling RH values higher than 37% increases, while in the current situation we have 35 – 37% of RH. There are no significant variations in the areas around the amphitheatre and CEIS (*figure 9.d*).

For detailed values, see Annex, Tables 13.1 and 13.2.

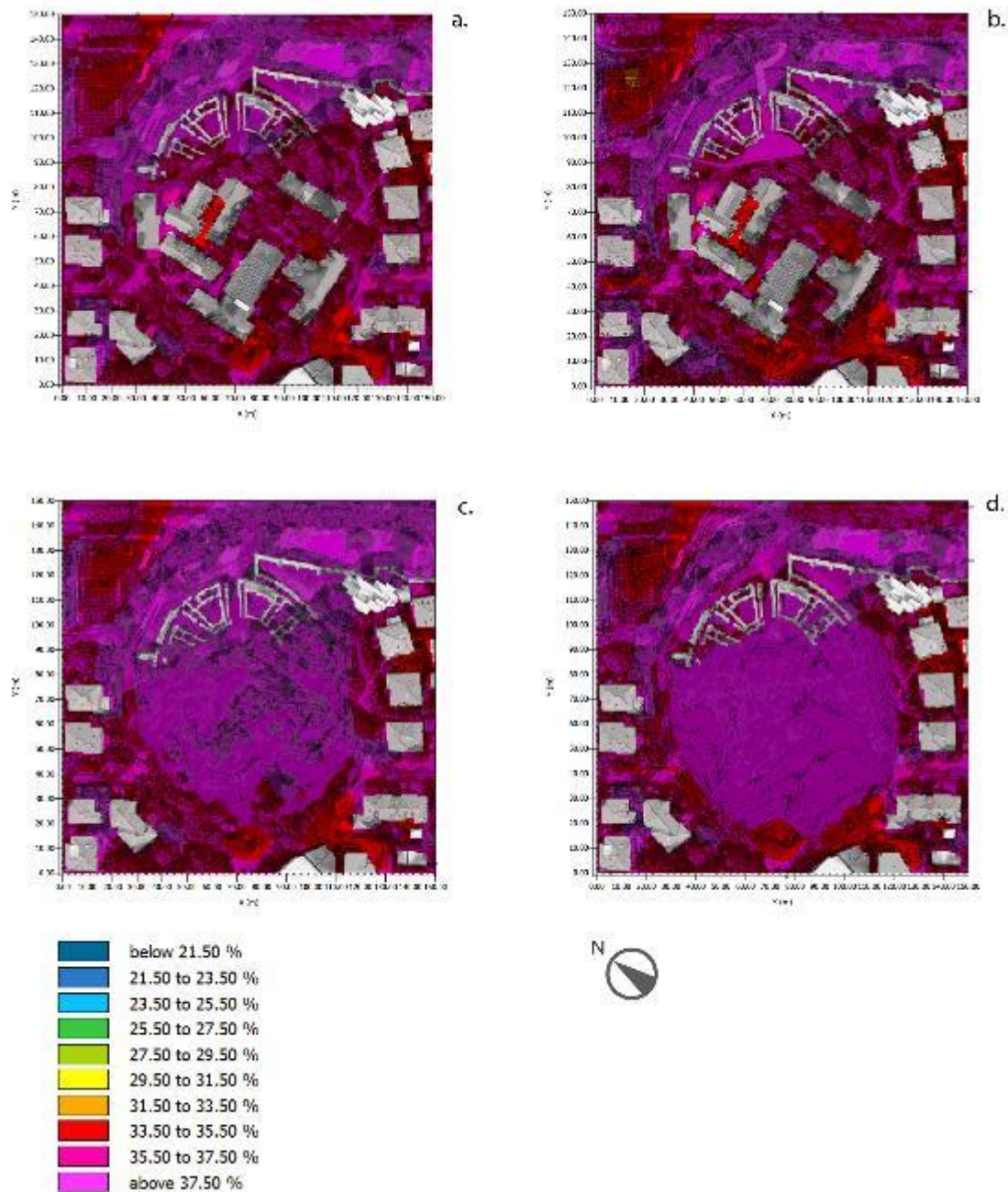


**Figura 9.** Small model: RH results at 14:00: (a) scenario 0, current state; (b) scenario 4; (c) scenario 5; (d) scenario 6.

OMM surface temperature scenarios, small area

*Scenario 0 small scale:* surface temperature reaches high values, especially in parking lots and along via Vezia; at 14:00, values above 50 ° C are registered there, while wooded areas maintain lower surface temperatures, of 28 - 32°C (*figure 10.a*).

*Scenario 4:* our project brings a significant surface temperature increase – at 14:00 we register values of 30 – 32°C in the arena, so 2 – 4°C higher than the current state ones. The values increase near the ruins and the CEIS, too (*figure 10.b*).

*Scenario 5:* positive effects are registered both for the CEIS and the ruins areas - at 14:00, the surface temperature in the CEIS area is 28 - 32°C, lower than the 40 - 44°C of the current state, and near the ruins the yellow-coloured areas (40 - 44°C) are smaller, favouring the light-green-coloured ones (36 - 40 ° C) (*figure 10.c*).

*Scenario 6:* we register positive effects thanks to the grass introduced – at 14:00, there are values of 28 – 32°C, significantly lower than the current state. The ruins, instead, suffer negative consequences due to the absence of trees: we reach 40 – 44°C in the arena and a temperature rising in between the remaining walls (*figure 10.d*).

*For detailed values, see Annex, Tables 14.1 and 14.2.*



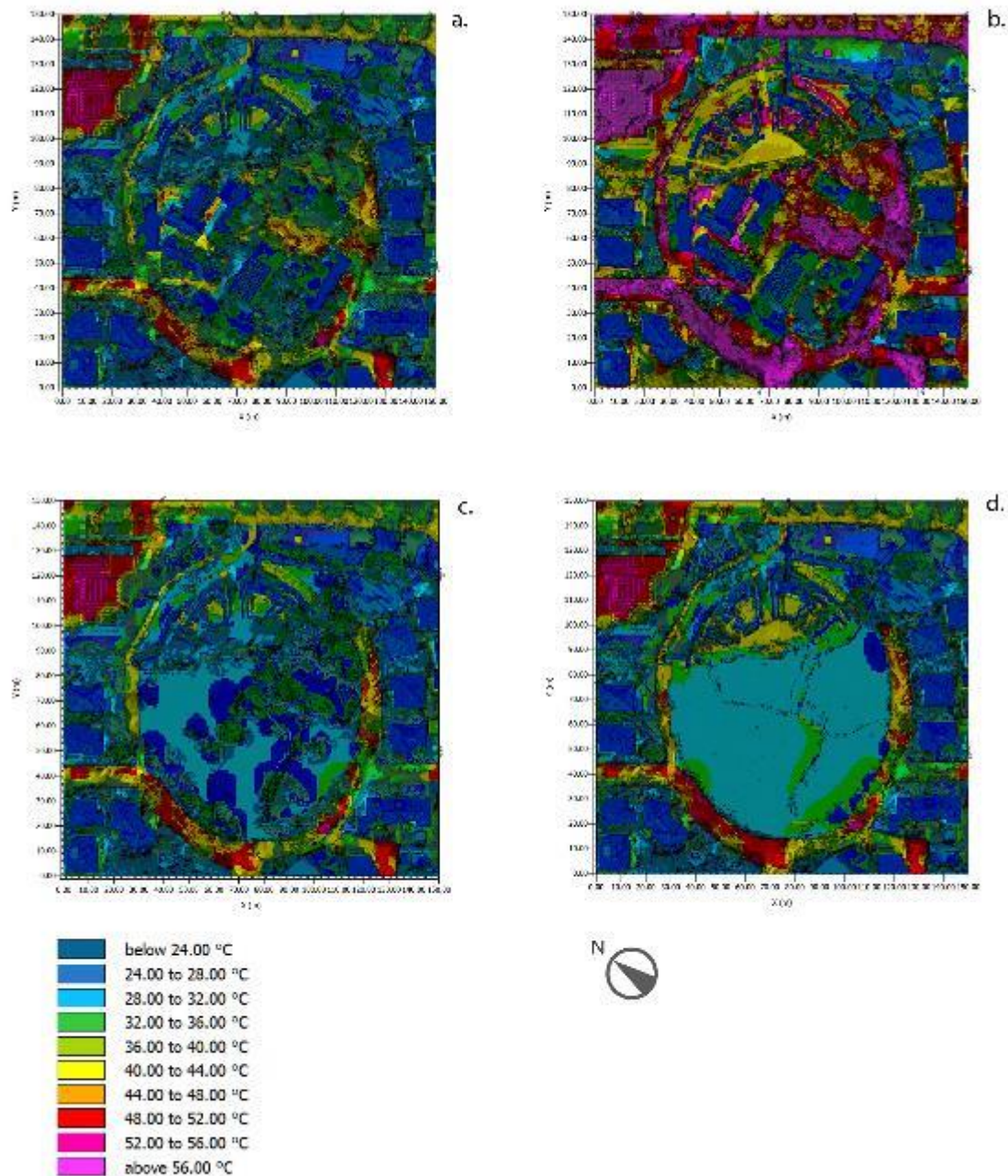


**Figure 10.** Small model: surface temperature results at 14:00: (a) scenario 0, current state; (b) scenario 4; (c) scenario 5; (d) scenario 6.

#### OMM PET scenarios, small model

*Scenario 0 small model:* in the early afternoon, we can identify the most critical area in-between the amphitheatre walls, reaching temperatures higher than 50°C (*extreme stress and heat stroke risk*). The situation in the arena is better, with 34 – 35°C (*slight heat and slight stress*), probably due to the shadows casted by the trees located in the CEIS area, protecting the area from excessive incident solar radiation (*figure 11.a*).

*Scenario 4:* in this project solution, at 14:00, red-coloured areas (47 - 50°C PET) are gathered in-between the remaining walls of the ruins, while in the arena we see an improvement, reaching 34 - 35 °C (*slightly warm and light stress conditions*). Along the entry path in compacted earth, the red-coloured area is wider than the actual state one, while there are better comfort levels alongside the hedge. There are no effects on the CEIS area or on the surroundings (*figure 11.b*).

*Scenario 5:* at 14:00, the CEIS area reaches 32°C PET near the trees, and 41 - 42°C PET, instead, in the sun-exposed areas - on one hand there are less shadows provided by buildings, but, on the other hand, red-coloured areas (47 - 50°C PET) are considerably reduced thanks to flooring change (*figure 11.c*).

*Scenario 6:* our project leads to lower comfort levels - at 14:00, we reach 44 °C PET in the CEIS area and very negative effects near the ruins - in the arena and in-between the remaining walls we reach 47 - 50°C PET. This can be a problem for visitors, especially in the morning and early afternoon (*figure 11.d*).

*For detailed values, see Annex, Tables 15.1 and 15.2.*

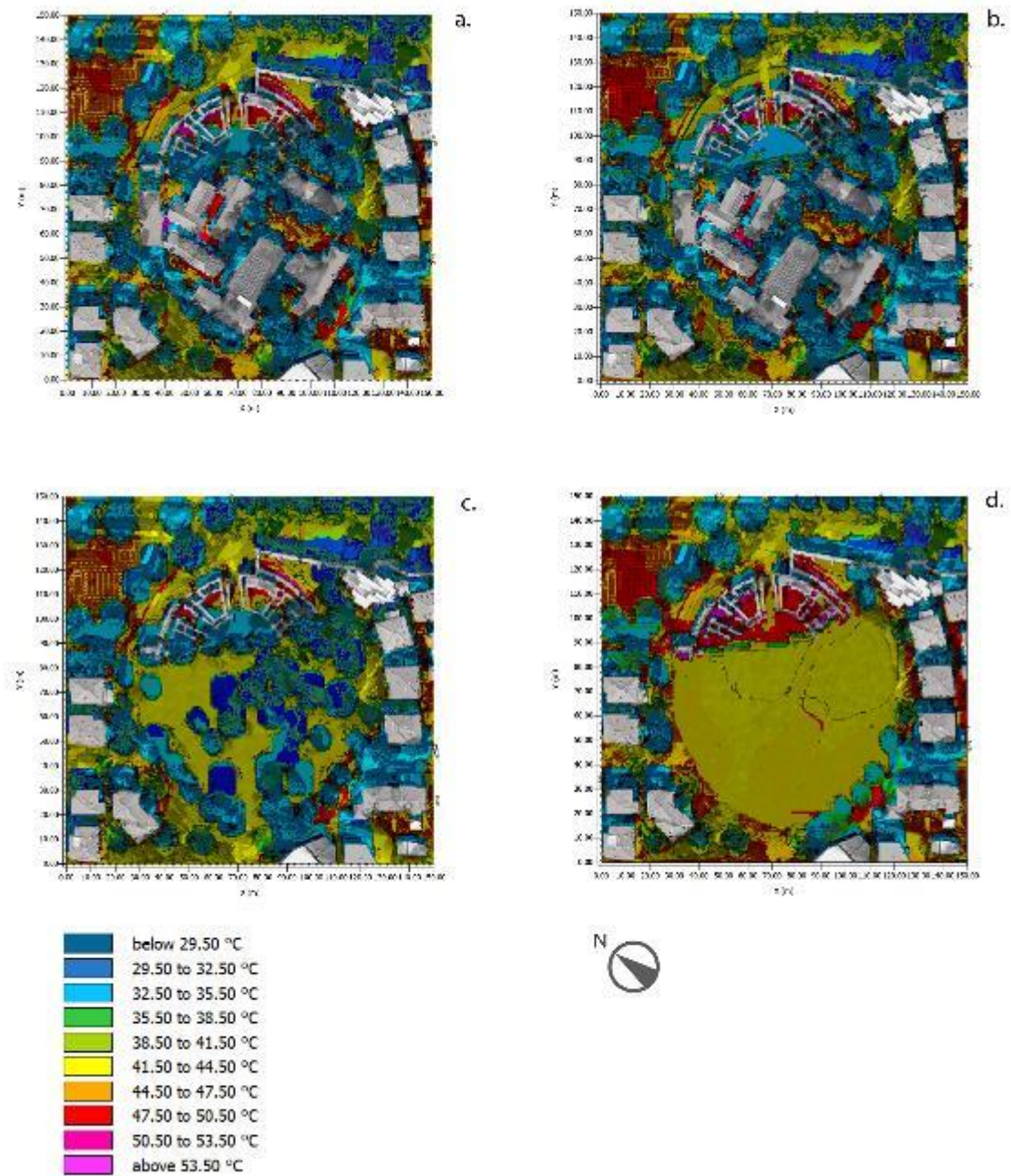


**Figure 11.** Small model: PET values at 14:00: (a) scenario 0, current state; (b) scenario 4; (c) scenario 5; (d) scenario 6.

### 5.3 Input-Output data comparison

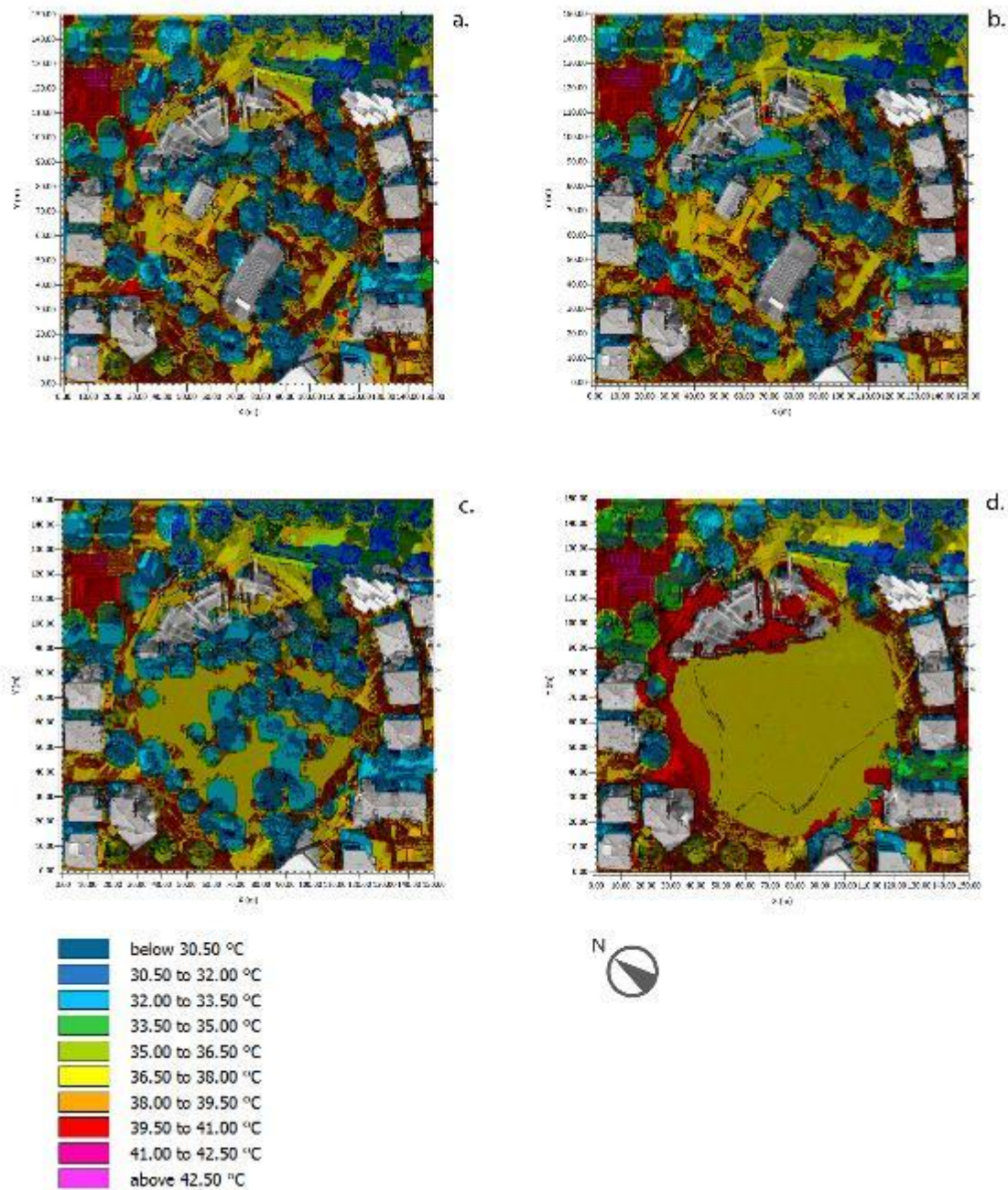
To better summarize the values we obtained for each physical parameter and to correlate said values with the scenario variables, we've set up this comparison table (*Table 16*), containing the mean hourly physical parameters registered at 14:00 (common to all scenarios) and the relevant variables:

Table 16. Summary of performed interventions and data related to the analysed physical variables.



	Input data				Output data (mean values by receptors)			
Scenarios	Tree nr.	Green area [%]	Water permeable area [%]	Mean reflectance	Air temp. [°C]	Relative humidity [%]	Surface temp. [°C]	PET [°C]*
0 large model	448	33.00	39.80	0.48	30.10	30.10	39.10	46.80
1	505	38.00	49.00	0.48	33.00	33.00	37.50	46.10
2	418	36.00	41.00	0.48	34.00	34.00	38.50	47.20
3	418	30.00	41.00	0.48	33.90	33.90	37.50	47.80
0 small model	64	33.00	33.40	0.33	33.00	36.30	39.20	43.40
4	66	32.00	33.60	0.33	33.70	36.90	39.60	42.40
5	64	55.00	54.30	0.33	33.40	36.60	39.10	43.20
6	38	55.00	54.30	0.33	33.80	36.20	39.60	45.40

\* all PET values correspond to a very hot sensation (Table 7) “*Estreme heat stress*”



**Figure 12.** Summary of performed solution and data related to the analysed physical variables, (a) for the large model, (b) for the small model

Figure 12 graphically shows the results reported in table 16. In both graphs of figure 12 the x-axis shows the PET values for each scenario, while the y-axis on the left represents the green and permeable area percentage, and the one on the right shows the tree number of each scenario. In this way, we can compare the effects of each project choice to the thermal comfort reached, expressed as mean PET value, all in a single image.

For the large model (a), the solutions planned for scenario 2 and 3 (elimination of the CEIS buildings) led to a slight increase in PET values, despite the increasing permeable area percentage. The role of green and permeable area in improving PET values is clear in scenario 1.

For the small model (b), the mean PET value is better, thanks to the dimensions of the considered area. The only scenario that led to lower PET values is the one with the less amount of trees (scenario 0). Scenario 5 is very similar to scenario 0, except for the green and permeable area percentage: we can clearly see the role played by the CEIS buildings. Lastly, scenario 4 appears to be the best one since it reduces the mean PET values by 1°C, thanks to the number of trees.

We can also clearly see that there is nonlinearity between the green or permeable area, the number of trees and thermal comfort. Generally, green areas and trees led to a better thermal comfort compared to non-permeable areas, such as asphalt, but there are other factors that affect thermal comfort and that aren't related to flooring or green areas, i.e. the sky factor and shadows variation due to the buildings removal in scenarios 2 and 3 and the role played by the context and the models dimension in relation to the intervention project.

The two graphs show that the mean PET values of the large model are higher compared to the ones of the small one, and that increasing the number of trees improves the PET values in scenario 1, but, with no variations in the tree amount, the buildings removal had a negative effect on the mean PET values. In the small model, the buildings role is balanced out by the increased extension of green areas and of the number of trees.

## 6 Discussion

From the large model scenarios data it appears clear that scenario 1, with added trees in the large parking lots, is very convenient regarding users comfort, since there are improvements in all the variables considered. In scenario 2 and 3, with the CEIS buildings and trees removal in favour of grass or mineral flooring, we can see negative effects not just in the immediate surroundings but in the context too. Grass is preferable to mineral flooring, but it is advisable to keep the existing trees or to consider planting new ones to improve thermal comfort.

According to the small model data, in scenario 4 there are no significant improvements in thermal comfort, except alongside the existing cycle path; the best project is the scenario 5 one: the CEIS buildings removal leads to a positive effects, especially regarding air temperature, surface temperature and relative humidity. Scenario 6, which also includes trees removal, on the other hand, has a negative effect on air and surface temperature, due to the decreased shadow amount.

None of the projects including modifications to the urban context affected the archaeological area. However, we can see that modifications in the archaeological and CEIS areas do affect the urban context too. We can therefore see the amphitheatre-CEIS area as a microclimatic unit of its own that is able to influence the surroundings; it's also important to emphasize that the CEIS buildings and trees somehow play the role of a barrier, protecting the archaeological area from the climatic stress coming from the city. This phenomenon can be graphically seen in figure 13.

The number of trees greatly contributes to thermal comfort improvement: we can see how in the current state, the vegetation keeps the surface temperature values low, even in private courts, as opposed to the high values reached by the paved areas. The scenarios that registered significant thermal comfort improvements are the ones with insertion of trees, shrubs or grassy areas or flooring: this is due to the role played by the vegetation in contrasting the air and surface temperature rising phenomena, thanks to foliage shading or evapotranspiration. Specifically, the more green areas are added, the greater the improvements, so we can see a direct correlation between vegetation increase and thermal comfort improvements (figure 12).

The most successful projects for thermal comfort improvements are scenario 1 and 5, respectively for the large model and the small one. Scenario 1 (figure 14.a) is characterized by 505 trees, 57 more than the actual ones, belonging to the species *Carpinus betulus* or *Fraxinus excelsior*. The green area percentage, including the inserted flowerbeds, is increased by 5%, reaching a total of 38%; we also report a permeable surface increase, going from 39.80% to 49%, thanks to the use of permeable and/or draining pavements

used in the parking lots in place of regular asphalt. Scenario 5 (*figure 14.b*) has no changes regarding the amount of trees (a total of 64, as in the current state), while there is 22% more green area, therefore reaching a 55%, thanks to the replacement of the CEIS buildings and gravel paving with grass. There is also a permeable surface percentage increase of 20.90%, reaching 54.30%.

The punctual, maximum, minimum and mean data we refer to in the text, are collected in tables that can be found in the Annex section; the four points A, B, C and D (that we refer to both in text and tables) are positioned respectively in the centre of the arena, in the Settebello parking, in the CEIS area and alongside the Margherita Zoebeli cycle path and are the receptors already mentioned in paragraph 4.1.1.

According to the observations made, tourists visits should not happen during the central hours of the day, since the simulations carried out at hour 12:00 and 14:00 report the most critical values for thermal comfort. Early morning and late afternoon are the most comfortable time of the day during a hot summer day.

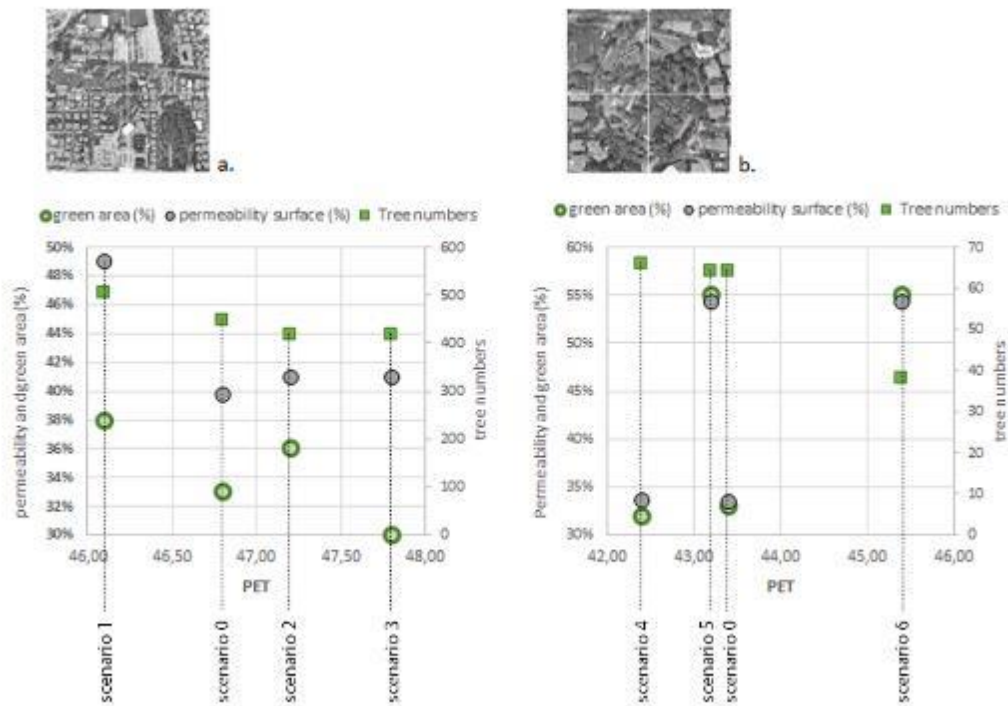


**Figure 13.** a) scenario 1 – scenario 0 air temperature absolute difference [ $^{\circ}\text{C}$ ] b) scenario 3 – scenario 0 air temperature difference [ $^{\circ}\text{C}$ ].

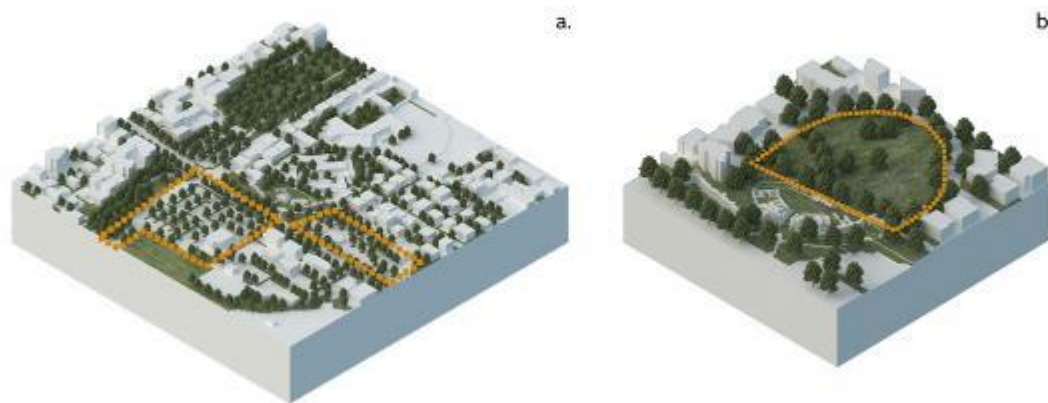


**Figure 14.** a) Scenario 1 b) Scenario 5

## 7 Conclusion

In conclusion, our research shows how the methodology we opted for can evaluate the role of vegetation in archaeological areas and how it affects the visitors/tourists thermal comfort by using PET analysis and microclimatic parameters (air temperature, relative humidity etc.). It appears clear that there is a correlation between the number of trees and the amount of green areas and the PET values registered. Despite PET values still being high, there was an improvement in the scenarios with more trees and green areas: it's safe to say there is an inverse proportionality. This is a good result, considering how little is known about archaeological areas and this aspect. Indeed, despite some limitation of the models, it appears clear that the simulated scenarios can be effectively used to study archaeological areas, since they allow to point out what kind of interventions are the better ones to optimize the thermal conditions of the area. This way we proved that vegetation doesn't necessarily have to be seen a danger for ruins, but it can also be an ally both for their preservation and for their fruition, therefore allowing us to share the knowledge and the history about their past.

The results we obtained and our data analysis can back up political decision-makers and designers, both for this specific case and for other archaeological areas: the tourists tour and the archaeological area fruition, together with green areas designing, can be planned not just to improve thermal comfort but also to facilitate the work of tour guides.

Moreover, our results can prove the effects of design choices on an urban plan scale, and the visitors thermal comfort on a smaller, more detailed scale.

Our research shows how model scale can affect the output interpretation when, as we proved in previous paragraphs, model at a different scales are related to each other, through calibration and receptors, and identified as microclimatic units.

The research methodology we adopted is replicable in other studies and adds an additional piece in the outdoor microclimate subject area, specifically, through the use of the ENVI-met software. This study area recently had a significant increase in research papers published on journals: the majority of them refer to case studies related to specific areas. Our area is a peculiar case, since it's an archaeological area addressed at two different scales.

Future studies could be carried on about evaluating the thermal comfort perception by comparing simulated PET values with questionnaires given to on-site visitors, to assess the perceived thermal sensation through the use of the *one-hour thermal acceptability* test, for more reliable and realistic results.

### Acknowledge

Special thanks to Professor Filippo Piva for his precious help with the vegetation and tree species, both already present in the area and used in the different scenarios and to dr. Marco Callisti for the data related the outdoor microclimate of the area.

### Nomenclature

ATR	Transient Acceptable Temperature Range
CEIS	Italian-Swiss Education Centre
CV (RMSE)	Coefficient of Variation of Root-Mean-Square Error
GRC	Green Coverage Ratio
LAD	Leaf Angle Distribution
LAI	Leaf Area Index
MBE	Mean Bias Error
OMM	Outdoor Microclimate Maps
PET	Physiologic Equivalent Temperature
PMV	Predicted Mean Vote
RH	Relative Humidity

### References

- [1] UNI 11182:2006, Beni culturali - Materiali lapidei naturali ed artificiali - Descrizione della forma di alterazione - Termini e definizioni, (2006).
- [2] ICOMOS, Illustrated Glossary on Stone Deterioration Patterns Glosario ilustrado de formas de deterioro de la piedra, Monum. y Sitios XV. (2011).
- [3] T.E. Morakinyo, K.K.L. Lau, C. Ren, E. Ng, Performance of Hong Kong's common trees species for outdoor temperature regulation, thermal comfort and energy saving, Build. Environ. 137 (2018) 157–170. <https://doi.org/10.1016/j.buildenv.2018.04.012>.
- [4] M. Fahmy, S. Sharples, M. Yahiya, LAI based trees selection for mid latitude urban developments: A microclimatic study in Cairo, Egypt, Build. Environ. (2010). <https://doi.org/10.1016/j.buildenv.2009.06.014>.
- [5] T. Zölch, M.A. Rahman, E. Pfeleiderer, G. Wagner, S. Pauleit, Designing public squares with green infrastructure to optimize human thermal comfort, Build. Environ. 149 (2019) 640–654. <https://doi.org/10.1016/j.buildenv.2018.12.051>.
- [6] A. Matzarakis, H. Mayer, M.G. Iziomon, Applications of a universal thermal index: Physiological equivalent temperature, Int. J. Biometeorol. (1999). <https://doi.org/10.1007/s004840050119>.
- [7] A. Matzarakis, B. Amelung, Physiological Equivalent Temperature as Indicator for Impacts of Climate Change on Thermal Comfort of Humans, Media. 30 (2008) 161–172. [https://doi.org/10.1007/978-1-4020-6877-5\\_10](https://doi.org/10.1007/978-1-4020-6877-5_10).
- [8] L. Zhang, Q. Zhan, Y. Lan, Effects of the tree distribution and species on outdoor environment conditions in a hot summer and cold winter zone: A case study in Wuhan residential quarters, Build. Environ. 130 (2018) 27–39. <https://doi.org/10.1016/j.buildenv.2017.12.014>.
- [9] M.F. Shahidan, P.J. Jones, J. Gwilliam, E. Salleh, An evaluation of outdoor and building environment cooling achieved through combination modification of trees with ground materials, Build. Environ. (2012). <https://doi.org/10.1016/j.buildenv.2012.07.012>.
- [10] W. Klemm, B.G. Heusinkveld, S. Lenzholzer, B. van Hove, Street greenery and its physical and psychological impact on thermal comfort, Landsc. Urban Plan. 138 (2015) 87–98. <https://doi.org/10.1016/j.landurbplan.2015.02.009>.
- [11] X. Yang, L. Zhao, M. Bruse, Q. Meng, Evaluation of a microclimate model for predicting the thermal



- behavior of different ground surfaces, *Build. Environ.* 60 (2013) 93–104. <https://doi.org/10.1016/j.buildenv.2012.11.008>.
- [12] F. Salata, I. Golasi, R. de Lieto Vollaro, A. de Lieto Vollaro, Urban microclimate and outdoor thermal comfort. A proper procedure to fit ENVI-met simulation outputs to experimental data, *Sustain. Cities Soc.* 26 (2016) 318–343. <https://doi.org/10.1016/j.scs.2016.07.005>.
- [13] G. Battista, E. Carnielo, R. De Lieto Vollaro, Thermal impact of a redeveloped area on localized urban microclimate: A case study in Rome, *Energy Build.* 133 (2016) 446–454. <https://doi.org/10.1016/j.enbuild.2016.10.004>.
- [14] S. Shooshtarian, Theoretical dimension of outdoor thermal comfort research, *Sustain. Cities Soc.* (2019). <https://doi.org/10.1016/j.scs.2019.101495>.
- [15] S. Zare, N. Hasheminezhad, K. Sarebanzadeh, F. Zolala, R. Hemmatjo, D. Hassanvand, Assessing thermal comfort in tourist attractions through objective and subjective procedures based on ISO 7730 standard: A field study, *Urban Clim.* (2018). <https://doi.org/10.1016/j.uclim.2018.08.001>.
- [16] P.K. Cheung, C.Y. Jim, Improved assessment of outdoor thermal comfort: 1-hour acceptable temperature range, *Build. Environ.* (2019). <https://doi.org/10.1016/j.buildenv.2019.01.057>.
- [17] A. Ugolini, T. Matteini, Trasformando lo sguardo. Il ruolo della vegetazione nella conservazione dei manufatti allo stato di rudere., in: *Eresia Ed Ortodossia Nel Restauro. Progett. e Realizz.*, Edizioni Arcadia ricerche, 2016.
- [18] A. Ugolini, T. Matteini, Design and active conservation of archaeological landscapes. New windows of research for interdisciplinary reading, in: *Conserv. e Valorizzazione Dei Siti Archeol. Approcci Sci. e Probl. Di Metod. Atti Del Convegno Di Stud. Bressanone 9 -12 Luglio 2013*, Edizioni Arcadia ricerche, Marghera - Venezia, 2013.
- [19] X. Luo, Z. Gu, T. Li, X. Meng, T. Ma, C. Yu, Environmental control strategies for the in situ preservation of unearthed relics in archaeology museums, *J. Cult. Herit.* (2015). <https://doi.org/10.1016/j.culher.2015.03.013>.
- [20] X. Luo, T. Wei, P. Song, Z. Wang, Z. Gu, Independent Environmental Control for Relics Preservation and Visitors' Thermal Comfort in Archaeology Museums, *Procedia Eng.* 205 (2017) 259–264. <https://doi.org/10.1016/j.proeng.2017.09.962>.
- [21] K. Fabbri, G. Canuti, A. Ugolini, A methodology to evaluate outdoor microclimate of the archaeological site and vegetation role: A case study of the Roman Villa in Russi (Italy), *Sustain. Cities Soc.* (2017). <https://doi.org/10.1016/j.scs.2017.07.020>.
- [22] W. Köppen, R. Geiger, Das Geographische System der Klimate, *Handb. Der Klimatologie.* (1936) 7–30. <https://doi.org/10.3354/cr01204>.
- [23] F.R. M. Kottek, J. Grieser, C. Beck, B. Rudolf, World map of the Köppen- Geiger climate classification updated, *Meteorol. Z.* 15 (2006) 259–263.
- [24] Meteoblue ([www.meteoblue.com](http://www.meteoblue.com)), (n.d.) 3171457.
- [25] A. Fontemaggi, O. Piolanti, Alla scoperta dell'anfiteatro romano: un luogo di spettacolo tra archeologia e storia, *Il Ponte Vecchio*, Cesena, 1999.
- [26] A. Ugolini, K. Fabbri, A. Lambertini, M. Maioli, T. Matteini, S. Morri, M.L. Stoppioni, *Ruderi, baracche, bambini - CEIS: Riflessioni a più voci su un'architettura speciale*, Altralinea Edizioni, 2017.
- [27] J. Gaspari, K. Fabbri, A Study on the Use of Outdoor Microclimate Map to Address Design Solutions for Urban Regeneration, *Energy Procedia.* 111 (2017) 500–509. <https://doi.org/10.1016/j.egypro.2017.03.212>.
- [28] Envi-met [www.envi-met.com](http://www.envi-met.com), (n.d.).
- [29] ARPAE Emilia Romagna, (Last accessed: August 2019) <http://www.smr.arpa.emr.it/dext3r/>, (2018).
- [30] ARPAER, Stazione meteo Rimini (Rimini Weather Station), (2019). <http://mcmeteo.altervista.org/>.
- [31] ANSI/ASHRAE, ASHRAE Guideline 14-2002 Measurement of Energy and Demand Savings, *Ashrae.* 8400 (2002) 170.
- [32] K. Fabbri, V. Costanzo, Drone-assisted infrared thermography for calibration of outdoor microclimate simulation models, *Sustain. Cities Soc.* in press (2019) 101855. <https://doi.org/10.1016/j.scs.2019.101855>.
- [33] S.N. Gosling, E.K. Bryce, P.G. Dixon, K.M.A. Gabriel, E.Y. Gosling, J.M. Hanes, D.M. Hondula, L. Liang,

P.A. Bustos Mac Lean, S. Muthers, S.T. Nascimento, M. Petralli, J.K. Vanos, E.R. Wanka, A glossary for biometeorology, 2014. <https://doi.org/10.1007/s00484-013-0729-9>.

- [34] R.F. Rupp, N.G. Vásquez, R. Lamberts, A review of human thermal comfort in the built environment, *Energy Build.* 105 (2015) 178–205. <https://doi.org/10.1016/j.enbuild.2015.07.047>.

## Annexs

TABLE 8.1: AIR TEMPERATURE LARGE AREA: Main results, concerning the critical hour (14:00).

SCENARIO NR.	AIR TEMPERATURE IN A	AIR TEMPERATURE IN B	AIR TEMPERATURE IN C	AIR TEMPERATURE IN D	MINIMUM AIR TEMPERATURE	MAXIMUM AIR TEMPERATURE
0	33.00 °C	35.00 °C	33.00 °C	33.00 °C	27.44 °C	39.42 °C
1	32.00 °C	32.00 °C	32.00 °C	32.00 °C	27.36 °C	38.74 °C
2	37.90 °C	35.50 °C	35.50 °C	33.90 °C	27.51 °C	40.46 °C
3	37.00 °C	34.50 °C	34.50 °C	34.50 °C	27.50 °C	40.39 °C

TABLE 8.2 AIR TEMPERATURE LARGE AREA: Secondary results concerning every analysed hour.

SCENARIO NR.	MEAN AIR TEMPERATURE h. 10:00	MEAN AIR TEMPERATURE h. 12:00	MEAN AIR TEMPERATURE h. 14:00	MEAN AIR TEMPERATURE h. 16:00
0	28.70 °C	29.90 °C	30.10 °C	29.60 °C
1	28.70 °C	31.30 °C	33.00 °C	33.90 °C
2	29.40 °C	32.20 °C	34.00 °C	34.70 °C
3	29.30 °C	32.20 °C	33.90 °C	34.60 °C

TABLE 9.1 RELATIVE HUMIDITY LARGE AREA: Main results, concerning the critical hour (14:00).

SCENARIO NR.	RELATIVE HUMIDITY IN A	RELATIVE HUMIDITY IN B	RELATIVE HUMIDITY IN C	RELATIVE HUMIDITY IN D	MINIMUM RELATIVE HUMIDITY	MAXIMUM RELATIVE HUMIDITY
0	37.50 %	29.50 %	39.50 %	33.50 %	24.01 %	46.39 %
1	37.50 %	42.50 %	37.50 %	37.50 %	26.96 %	47.72 %
2	26.50 %	32.50 %	29.50 %	35.50 %	23.68 %	45.04 %
3	27.50 %	32.50 %	32.50 %	35.00 %	23.75 %	45.52 %

TABLE 9.2 RELATIVE HUMIDITY LARGE AREA: Secondary results concerning every analysed hour.

SCENARIO NR.	MEAN RELATIVE HUMIDITY h. 10:00	MEAN RELATIVE HUMIDITY h. 12:00	MEAN RELATIVE HUMIDITY h. 14:00	MEAN RELATIVE HUMIDITY h. 16:00
0	33.90 %	34.50 %	30.10 %	29.90 %
1	35.80 %	36.60 %	33.00 %	31.00 %
2	33.30 %	34.00 %	34.00 %	29.20 %
3	33.40 %	34.10 %	33.90 %	29.40 %

TABLE 10.1 SURFACE TEMPERATURE LARGE AREA: Main results, concerning the critical hour (14:00).

SCENARIO NR.	T. SURFACE IN A	T. SURFACE IN B	T. SURFACE IN C	T. SURFACE IN D	MINIMUM T. SURFACE	MAXIMUM T. SURFACE
0	28.50 °C	48.50 °C	33.50 °C	28.50 °C	19.85 °C	58.44 °C
1	30.50 °C	36.50 °C	30.50 °C	30.50 °C	19.85 °C	55.21 °C
2	46.50 °C	46.50 °C	39.50 °C	39.50 °C	19.85 °C	57.15 °C
3	46.50 °C	48.50 °C	43.50 °C	38.50 °C	19.85 °C	57.07 °C

TABLE 10.2 SURFACE TEMPERATURE LARGE AREA: Secondary results concerning every analysed hour.

SCENARIO NR.	MEAN T.S. h. 10:00	MEAN T.S. h. 12:00	MEAN T.S. h. 14:00	MEAN T.S. h. 16:00
0	35.70 °C	37.90 °C	39.10 °C	37.50 °C
1	34.40 °C	38.00 °C	37.50 °C	36.30 °C
2	36.20 °C	37.60 °C	38.50 °C	37.40 °C
3	36.10 °C	38.70 °C	37.50 °C	37.70 °C

TABLE 11.1 PET LARGE AREA: Main results, concerning the critical hour (14:00).

SCENARIO NR.	PET IN A	PET IN B	PET IN C	PET IN D	MINIMUM PET	MAXIMUM PET
0	37.50 °C	47.50 °C	36.50 °C	36.50 °C	34.56 °C	59.00 °C
1	37.50 °C	42.50 °C	37.50 °C	42.50 °C	33.90 °C	58.40 °C
2	43.50 °C	46.50 °C	43.50 °C	43.50 °C	35.15 °C	59.40 °C
3	46.50 °C	46.50 °C	46.50 °C	46.50 °C	35.04 °C	60.60 °C

TABLE 11.2 PET LARGE AREA: Secondary results concerning every analysed hour.

SCENARIO NR.	MEAN PET h. 10:00	MEAN PET h. 12:00	MEAN PET h. 14:00	MEAN PET h. 16:00
0	44.40 °C	46.20 °C	46.80 °C	45.80 °C
1	43.70 °C	45.20 °C	46.10 °C	45.20 °C
2	45.10 °C	46.20 °C	47.20 °C	45.80 °C
3	45.30 °C	47.40 °C	47.80 °C	47.00 °C

TABLE 12.1 AIR TEMPERATURE SMALL AREA: Main results, concerning the critical hour (14:00).

SCENARIO NR.	AIR TEMPERATURE IN A	AIR TEMPERATURE IN C	AIR TEMPERATURE IN D	MINIMUM AIR TEMPERATURE	MAXIMUM AIR TEMPERATURE
0	33.00 °C	33.00 °C	33.00 °C	32.38 °C	35.04 °C
4	33.00 °C	33.00 °C	32.50 °C	31.95 °C	35.51 °C
5	32.00 °C	32.50 °C	32.50 °C	31.63 °C	34.89 °C
6	33.00 °C	33.00 °C	33.00 °C	32.32 °C	35.12 °C

TABLE 12.2 AIR TEMPERATURE SMALL AREA: Secondary results concerning every analysed hour.

SCENARIO NR.	MEAN A. T. h. 08:00	MEAN A. T. h. 10:00	MEAN A. T. h. 12:00	MEAN A. T. h. 14:00	MEAN A. T. h. 16:00	MEAN A. T. h. 18:00
0	31.60 °C	33.00 °C	33.70 °C	33.00 °C	33.50 °C	32.90 °C
4	31.70 °C	33.10 °C	33.90 °C	33.70 °C	33.60 °C	32.90 °C
5	31.50 °C	33.00 °C	33.70 °C	33.40 °C	33.30 °C	32.70 °C
6	31.80 °C	33.40 °C	34.10 °C	33.80 °C	33.70 °C	33.00 °C

TABLE 13.1 RELATIVE HUMIDITY SMALL AREA: Main results, concerning the critical hour (14:00).

SCENARIO NR.	RELATIVE HUMIDITY IN A	RELATIVE HUMIDITY IN C	RELATIVE HUMIDTY IN D	MINIMUM RELATIVE HUMIDITY	MAXIMUM RELATIVE HUMIDITY
0	37.50 %	35.50 %	37.50 %	33.69 %	38.85 %
4	38.00 %	36.00 %	38.50 %	33.69 %	40.73 %

5	39.00 %	39.00 %	39.00 %	33.88 %	40.86 %
6	37.50 %	37.50 %	37.50 %	33.81 %	39.68 %

TABLE 13.2 RELATIVE HUMIDITY SMALL AREA: Secondary results concerning every analysed hour.

SCENARIO NR.	MEAN R.H. h. 08:00	MEAN R.H. h. 10:00	MEAN R.H. h. 12:00	MEAN R.H. h. 14:00	MEAN R.H. h. 16:00	MEAN R.H. h. 18:00
0	22.50 %	29.00 %	33.80 %	36.30 %	28.50 %	30.50 %
4	22.00 %	29.40 %	34.50 %	36.90 %	28.30 %	30.40 %
5	22.50 %	29.00 %	33.80 %	36.60 %	28.80 %	30.80 %
6	21.80 %	28.40 %	33.70 %	36.20 %	27.90 %	30.10 %

TABLE 14.1 SURFACE TEMPERATURE SMALL AREA: Main results, concerning the critical hour (14:00).

SCENARIO NR.	T. SURFACE IN A	T. SURFACE IN C	T. SURFACE IN D	MINIMUM T. SURFACE	MAXIMUM T. SURFACE
0	30.00 °C	30.00 °C	30.00 °C	22.67 °C	55.77 °C
4	32.00 °C	36.00 °C	32.00 °C	22.59 °C	56.55 °C
5	32.00 °C	32.00 °C	32.00 °C	22.57 °C	55.51 °C
6	40.00 °C	30.00 °C	35.00 °C	19.85 °C	56.24 °C

TABLE 14.2 SURFACE TEMPERATURE SMALL AREA: Secondary results concerning every analysed hour.

SCENARIO NR.	MEAN T. S. h. 08:00	MEAN T. S. h. 10:00	MEAN T. S. h. 12:00	MEAN T. S. h. 14:00	MEAN T. S. h. 16:00	MEAN T. S. h. 18:00
0	28.40 °C	37.00 °C	38.70 °C	39.20 °C	38.30 °C	34.60 °C
4	27.80 °C	36.50 °C	39.60 °C	39.60 °C	38.30 °C	34.00 °C
5	27.90 °C	37.10 °C	39.00 °C	39.10 °C	38.20 °C	34.50 °C
6	28.00 °C	38.40 °C	40.60 °C	39.60 °C	38.70 °C	34.40 °C

TABLE 15.1 PET SMALL AREA: Main results, concerning the critical hour (14:00).

SCENARIO NR.	PET IN A	PET IN C	PET IN D	MINIMUM PET	MAXIMUM PET
0	34.50 °C	34.50 °C	42.50 °C	30.56 °C	56.20 °C
4	35.50 °C	35.50 °C	41.50 °C	30.84 °C	54.00 °C
5	35.50 °C	35.50 °C	41.50 °C	29.88 °C	55.40 °C
6	49.00 °C	44.00 °C	44.00 °C	31.60 °C	57.00 °C

TABLE 15.2 PET SMALL AREA: Secondary results concerning every analysed hour.

SCENARIO NR.	MEAN PET h. 08:00	MEAN PET h. 10:00	MEAN PET h. 12:00	MEAN PET h. 14:00	MEAN PET h. 16:00	MEAN PET h. 18:00
0	40.10 °C	42.40 °C	42.20 °C	43.40 °C	42.30 °C	35.80 °C
4	38.90 °C	41.70 °C	42.50 °C	42.40 °C	41.80 °C	35.90 °C
5	40.20 °C	42.60 °C	42.20 °C	43.20 °C	43.30 °C	35.60 °C
6	41.30 °C	44.10 °C	44.30 °C	45.40 °C	45.50 °C	36.80 °C